Electronic Supplementary Information

Quest for 9-connected robust metal-organic framework platforms on the base of [M_3(O/OH)$(COO)_6$(pyridine)$_3$] cluster as excellent gas separation and asymmetric supercapacitor materials

Ying-Ying Xue, Shu-Ni Li, Yu-Cheng Jiang, Man-Cheng Hu, Quan-Guo Zhai*

Key Laboratory of Macromolecular Science of Shaanxi Province,

Key Laboratory of Applied Surface and Colloid Chemistry, Ministry of Education,

School of Chemistry & Chemical Engineering,

Shaanxi Normal University, Xi'an, Shaanxi, 710062, China

*E-mail: zhaiqg@snnu.edu.cn

Table S1. Crystal data and structure refinements for SNNU-51, SNNU-52 and SNNU-54.

Compound	SNNU-51 CCDC 1866054	SNNU-52 CCDC 1866055	SNNU-54 CCDC 1866056
Empirical formula	$C_{102}H_{60}Co_6N_{18}O_{25}$	$C_{102}H_{60}N_{18}Ni_6O_{25}$	$C_{96}H_{54}Co_6N_{24}O_{25}$
Formula weight	2291.26	2289.94	2297.21
Crystal system	Hexagonal	Hexagonal	Hexagonal
Space group	*P*6(3)/*m*	*P*6(3)/*m*	*P*-6*c*2
a (Å)	19.4081(15)	19.2359(13)	19.2411(6)
b (Å)	19.4081(15)	19.2359(13)	19.2411(6)
c (Å)	24.197(2)	24.063(2)	23.8936(11)
α (deg)	90	90	90
β (deg)	90	90	90
γ (deg)	120	120	120
V (Å^3)	7893.4(11)	7710.9(10)	7660.8(5)
Z	2	2	2
D_{calcd}(Mg·m^{-3})	0.964	0.986	0.996
μ(mm^{-1})	5.278	1.258	5.452
F(000)	2320	2332	2320
ϑ for data collection (deg)	2.63 to 66.04	2.65 to 66.05	2.65 to 66.00
Reflections collected/unique	18209 / 4711	17650 / 4615	17415 / 4548
R(int)	0.1297	0.1097	0.1285
parameters	237	237	236
GOF on F^2	0.968	0.900	0.972
R_1[a], wR_2 [I > 2δ (I)]	0.0594，0.0836	0.0714, 0.1662	0.0759, 0.1939
R_1, wR_2 (all data)	0.1003, 0.0901	0.1218, 0.1893	0.0915, 0.2043
ρ_{fin}(max/min) (e·Å^{-3})	0.403 /-2.327	0.37 /-2.84	0.42/-1.49

Table S2. Selected bonded lengths (Å) and angles (°) for SNNU-51.

Co(1)-O(5)	2.0376(10)	O(1)-Co(2)-N(1)#2	100.75(13)
Co(1)-O(3)#1	2.095(3)	O(1)#2-Co(2)-N(1)	100.75(13)
Co(1)-O(4)#1	2.104(3)	O(1)-Co(2)-N(1)	79.25(13)
Co(2)-O(1)#2	2.066(3)	N(1)#2-Co(2)-N(1)	180.00(18)
Co(1)-N(2)	2.138(5)	N(1)#2-Co(2)-N(3)	84.02(15)
Co(2)-N(1)#2	2.104(4)	O(1)#2-Co(2)-N(3)#2	89.08(13)
Co(2)-N(3)#2	2.215(4)	O(1)-Co(2)-N(3)#2	90.92(14)
O(5)-Co(1)-O(3)#1	90.31(9)	N(1)#2-Co(2)-N(3)#2	95.98(15)
O(3)-Co(1)-O(3)#1	94.83(19)	N(1)-Co(2)-N(3)#2	84.02(15)
O(5)-Co(1)-O(4)#1	93.91(10)	N(3)-Co(2)-N(3)#2	180.000(1)
O(3)-Co(1)-O(4)#1	175.73(13)	Co(1)#3-O(5)-Co(1)#4	120.000(1)
O(3)#1-Co(1)-O(4)#1	84.52(13)	O(1)#2-Co(2)-O(1)	180.000(1)
O(4)#1-Co(1)-O(4)	95.82(19)	O(1)#2-Co(2)-N(1)#2	79.25(13)
O(5)-Co(1)-N(2)	177.89(16)		
O(3)#1-Co(1)-N(2)	88.26(14)		
O(4)#1-Co(1)-N(2)	87.51(14)		

Symmetry codes: #1 x,y,-z+1/2; #2 -x+1,-y+1,-z+1; #3 -x+y,-x+1,z; #4 -y+1,x-y+1,z; #5 x-y,x,-z+1; #6 y,-x+y,-z+1.

Table S3. Selected bonded lengths (Å) and angles (°) for SNNU-52.

Ni(1)-O(5)	2.0131(11)	N(1)#2-Ni(2)-O(1)	98.97(15)
Ni(1)-O(4)#1	2.052(3)	O(1)#2-Ni(2)-O(1)	180.00(19)
Ni(1)-O(3)#1	2.060(3)	N(1)#2-Ni(2)-N(3)#3	84.53(17)
Ni(2)-O(1)#2	2.053(4)	O(1)#2-Ni(2)-N(3)#3	90.62(15)
Ni(1)-N(2)	2.078(5)	O(1)-Ni(2)-N(3)#3	89.38(15)
Ni(2)-N(1)#2	2.039(4)	N(1)-Ni(2)-N(3)#4	84.53(17)
Ni(2)-N(3)#4	2.137(4)	N(1)#2-Ni(2)-N(3)#4	95.47(17)
O(5)-Ni(1)-O(4)#1	90.67(10)	O(1)#2-Ni(2)-N(3)#4	89.38(15)
O(4)#1-Ni(1)-O(4)	95.0(2)	O(1)-Ni(2)-N(3)#4	90.62(15)
O(4)#1-Ni(1)-O(3)	175.85(15)	N(3)#3-Ni(2)-N(3)#4	180.0(3)
O(5)-Ni(1)-O(3)#1	93.47(10)		
O(4)#1-Ni(1)-O(3)#1	84.64(14)		
O(4)-Ni(1)-O(3)#1	175.85(15)		
O(3)-Ni(1)-O(3)#1	95.4(2)		
O(5)-Ni(1)-N(2)	178.43(17)		
O(4)#1-Ni(1)-N(2)	88.27(15)		
O(3)#1-Ni(1)-N(2)	87.59(14)		
N(1)-Ni(2)-N(1)#2	180.0		
N(1)-Ni(2)-O(1)#2	98.97(15)		
N(1)#2-Ni(2)-O(1)#2	81.03(15)		

Symmetry codes: #1 x,y,-z+1/2; #2 -x,-y+1,-z; #3 -y,x-y,z; #4 y,-x+y+1,-z; #5 -x+y,-x,z; #6 -y+1,x-y+1,z; #7 -x+y,-x+1,-z+1/2; #8 -x+y,-x+1,z

Table S4. Selected bonded lengths (Å) and angles (°) for SNNU-54.

Co(1)-O(5)	2.0231(12)	N(5)#5-Co(2)-N(5)#6	95.4(4)
Co(1)-O(4)#2	2.086(5)	O(1)#4-Co(2)-N(1)#4	78.62(19)
Co(1)-O(3)#3	2.119(5)	O(1)-Co(2)-N(1)#4	96.5(2)
Co(2)-O(1)#4	2.036(5)	N(5)#5-Co(2)-N(1)#4	87.5(2)
Co(1)-N(2)	2.133(7)	N(5)#6-Co(2)-N(1)#4	167.6(2)
Co(2)-N(5)#6	2.152(6)	O(1)#4-Co(2)-N(1)	96.5(2)
Co(2)-N(1)#4	2.180(6)	N(5)#5-Co(2)-N(1)	167.6(2)
O(5)-Co(1)-O(4)#2	94.02(14)	N(5)#6-Co(2)-N(1)	87.5(2)
O(4)#1-Co(1)-O(4)#2	93.6(3)	N(1)#4-Co(2)-N(1)	92.4(3)
O(4)#1-Co(1)-O(3)	87.22(18)	Co(1)#2-O(5)-Co(1)#8	120.0
O(5)-Co(1)-O(3)#3	91.87(15)	Co(1)-O(5)-Co(1)#8	120.0
O(4)#1-Co(1)-O(3)#3	173.97(19)		
O(4)#2-Co(1)-O(3)#3	87.22(18)		
O(3)-Co(1)-O(3)#3	91.3(3)		
O(5)-Co(1)-N(2)	175.7(3)		
O(4)#2-Co(1)-N(2)	88.9(2)		
O(3)#3-Co(1)-N(2)	85.1(2)		
O(1)#4-Co(2)-O(1)	173.1(3)		
O(1)#4-Co(2)-N(5)#5	95.6(2)		
O(1)-Co(2)-N(5)#5	89.0(2)		
O(1)#4-Co(2)-N(5)#6	89.0(2)		
O(1)-Co(2)-N(5)#6	95.6(2)		

Symmetry codes: #1 -x+y+1,-x+2,z; #2 -x+y+1,-x+2,-z+3/2; #3 x,y,-z+3/2; #4 -x+y+1,y,-z+2; #5 -y+1,-x+1,z+1/2; #6 -x+y+1,-x+1,-z+3/2; #7 -y+1,x-y,-z+3/2; #8 -y+2,x-y+1,z.

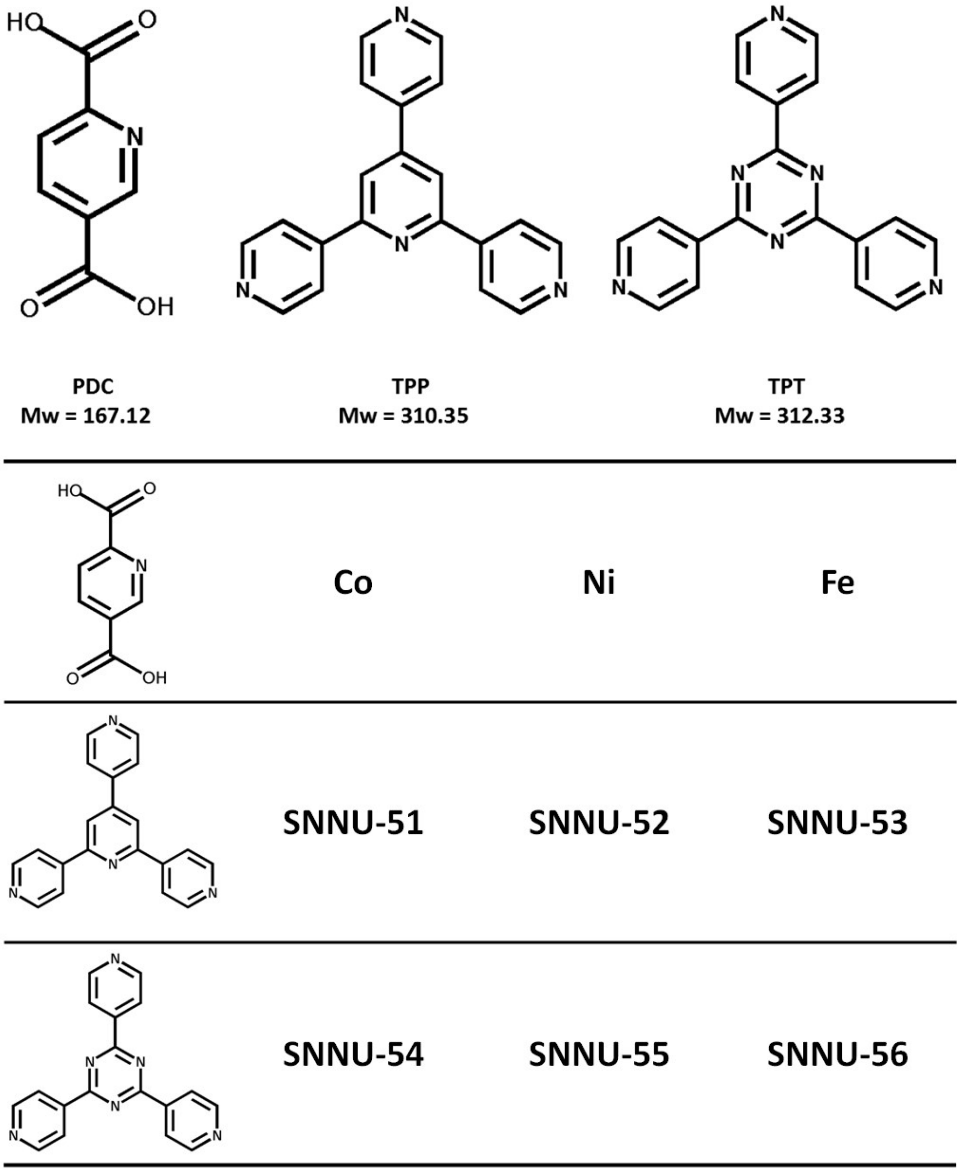

Figure S1. Molecular drawing of ligands and various ligand combinations for SNNU-51-56.

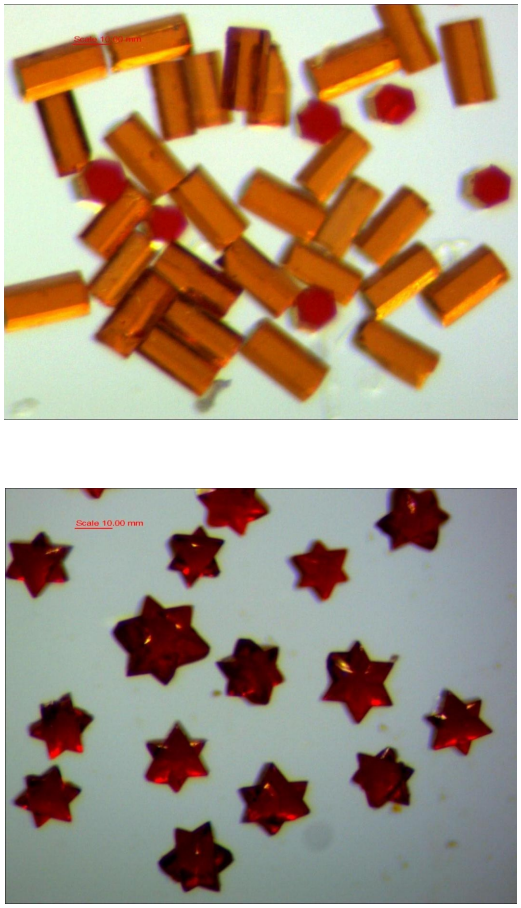

Figure S2. The photo pictures of single crystals for SNNU-51 (top) and SNNU-54 (bottom).

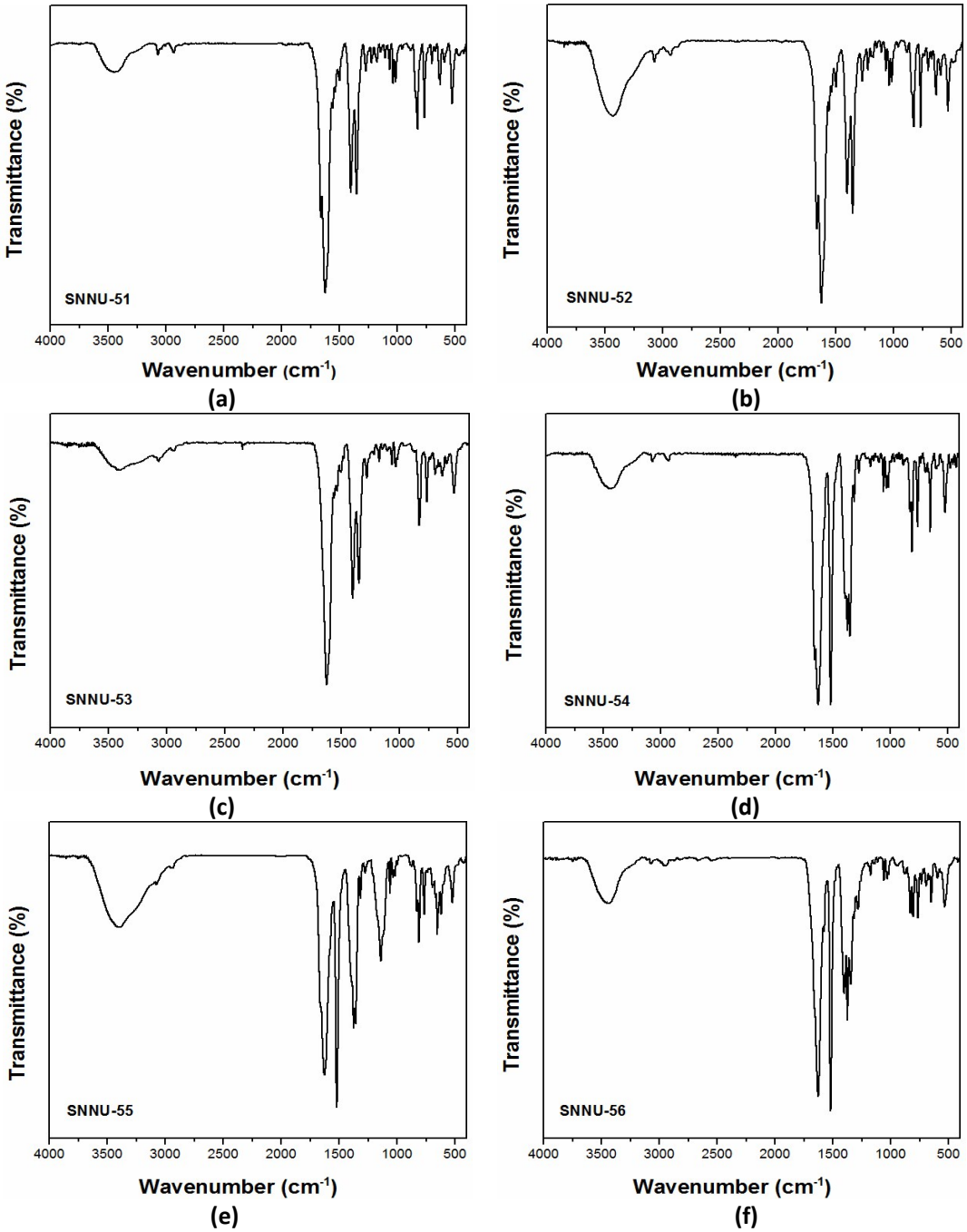

Figure S3. FT-IR spectra of SNNU-51-56.

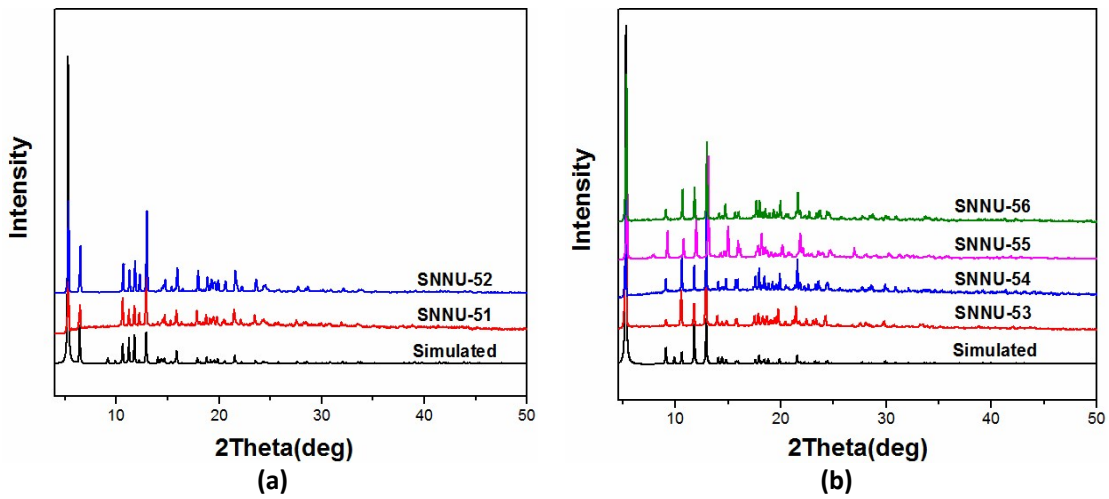

Figure S4. The simulated and experimental PXRD patterns for SNNU-51-56.

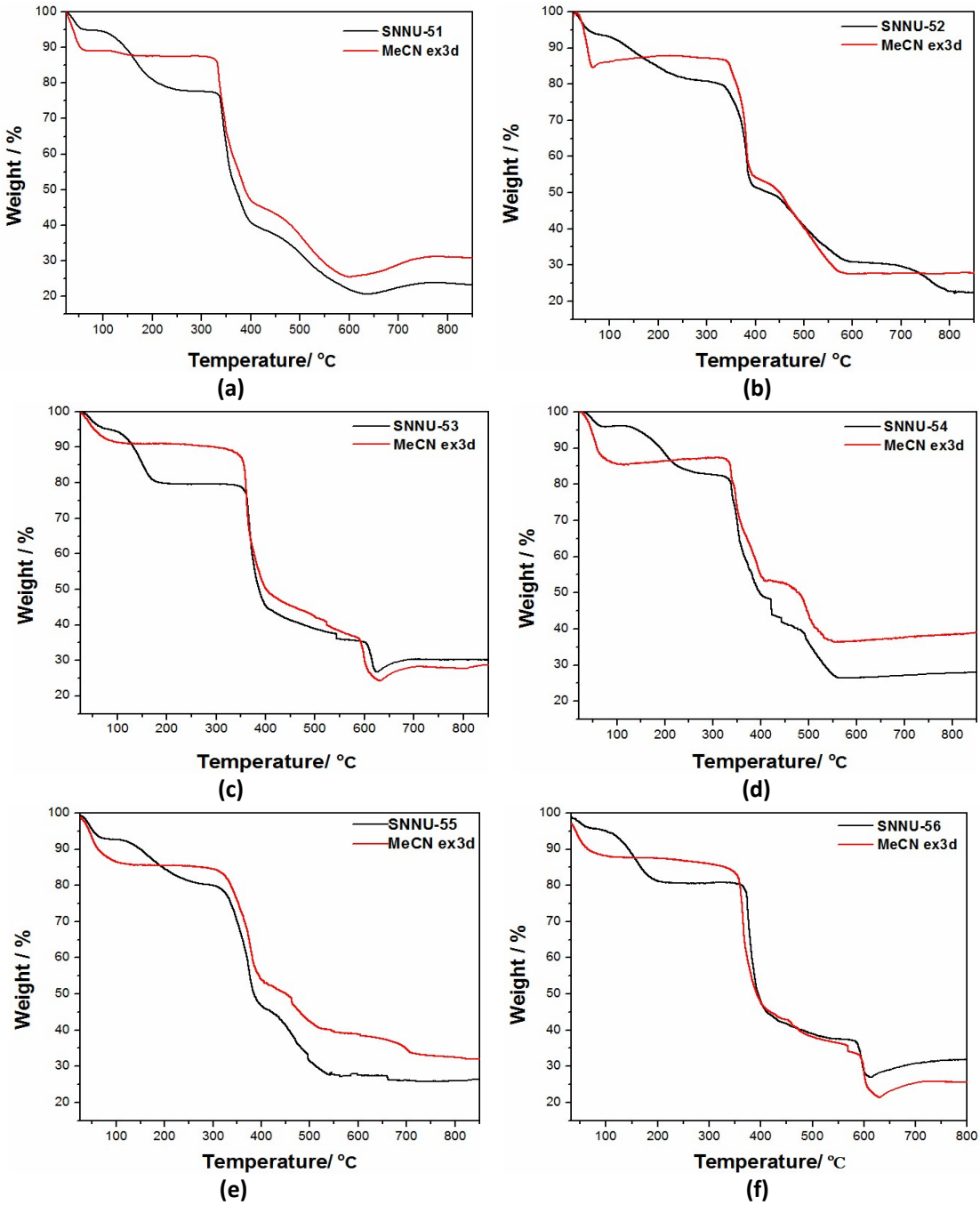

Figure S5. Thermogravimetric analyses (TGA) curves for the as-synthesized and activated samples of all compounds.

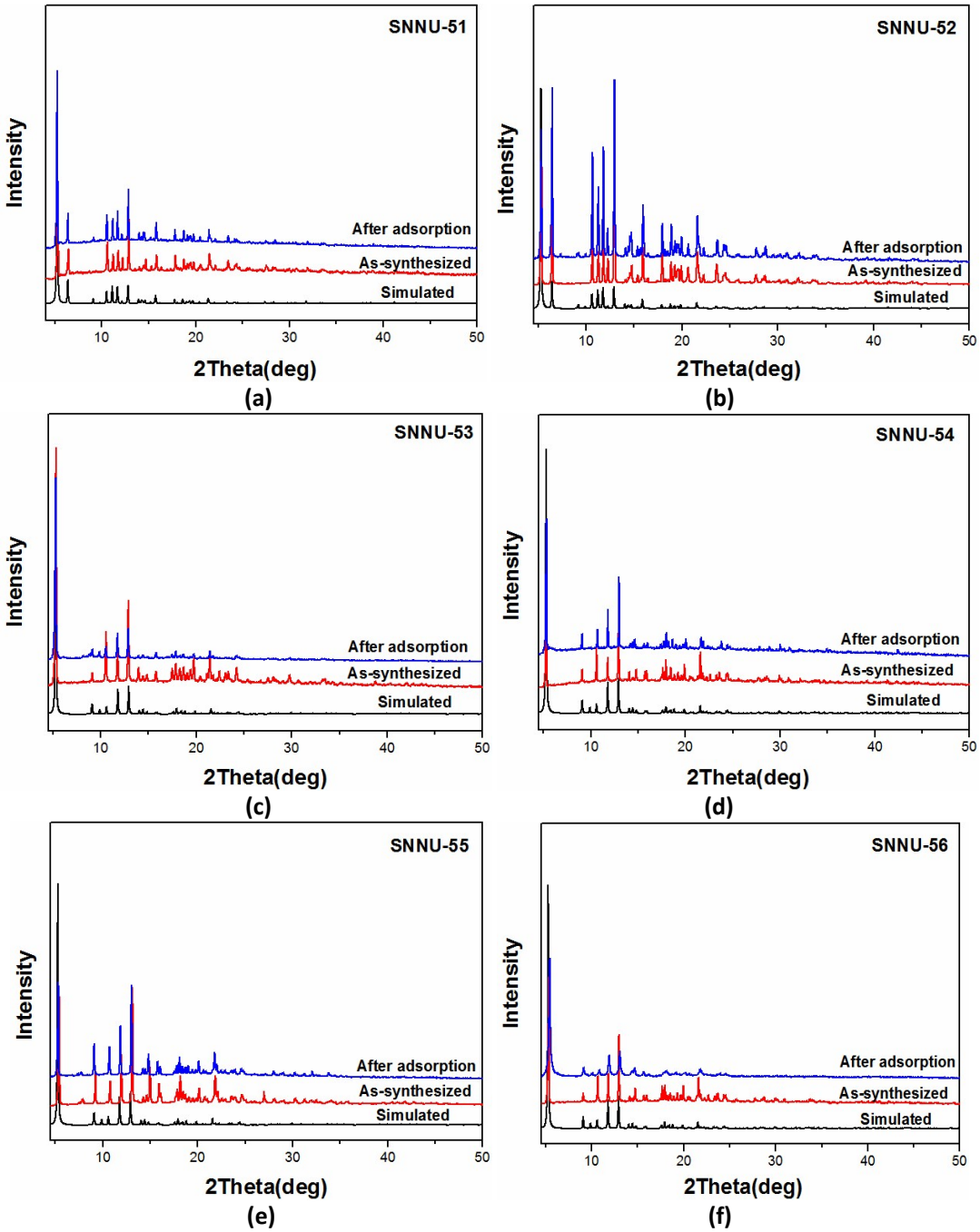

Figure S6. PXRD patterns for all MOFs after gas adsorption experiments.

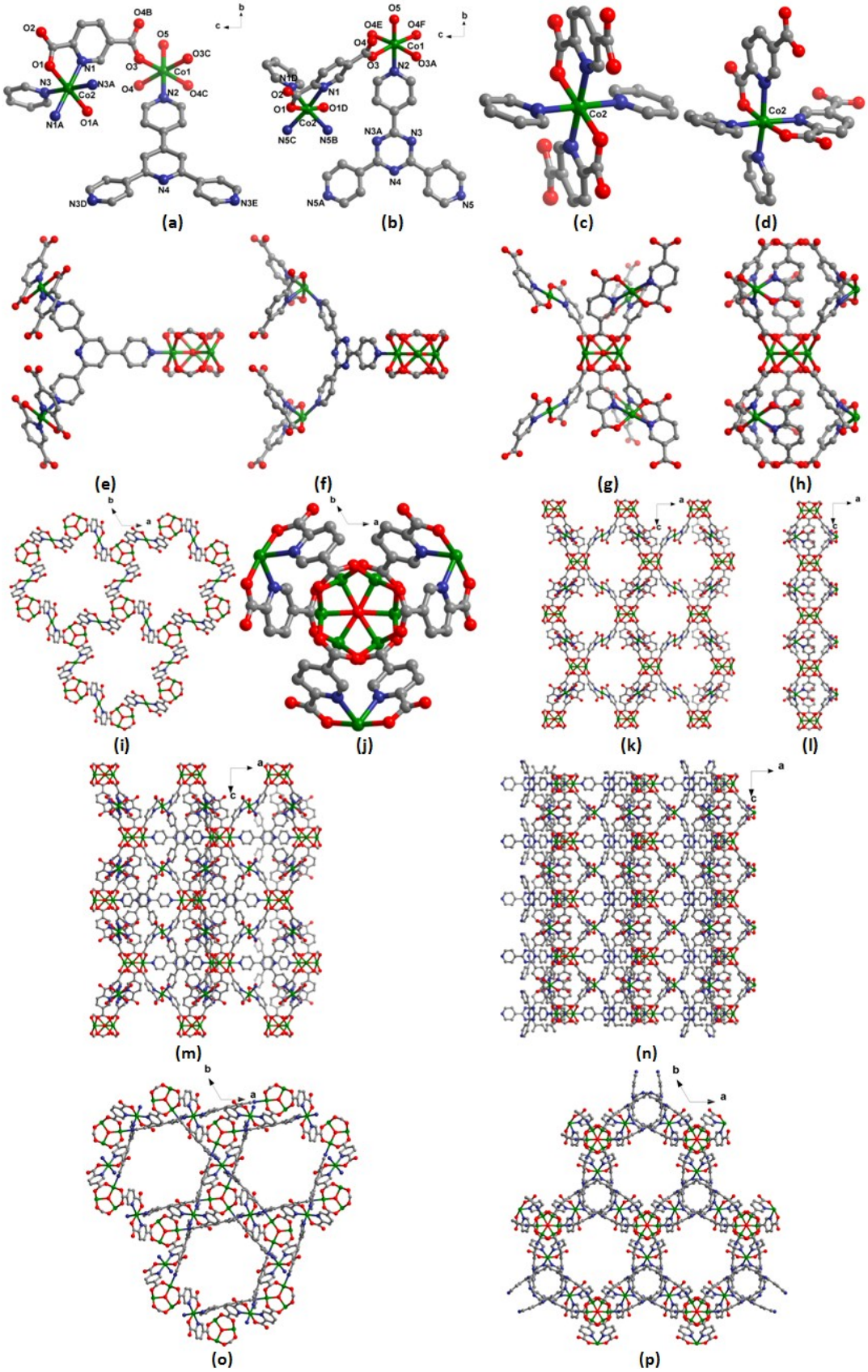

Figure S7. The structural details of SNNU-51 (a, c, e, g, i, k, m and o) and SNNU-54 (b, d, f, h, j, l, n p), which represent two types of new 9-c MOFs in this work.

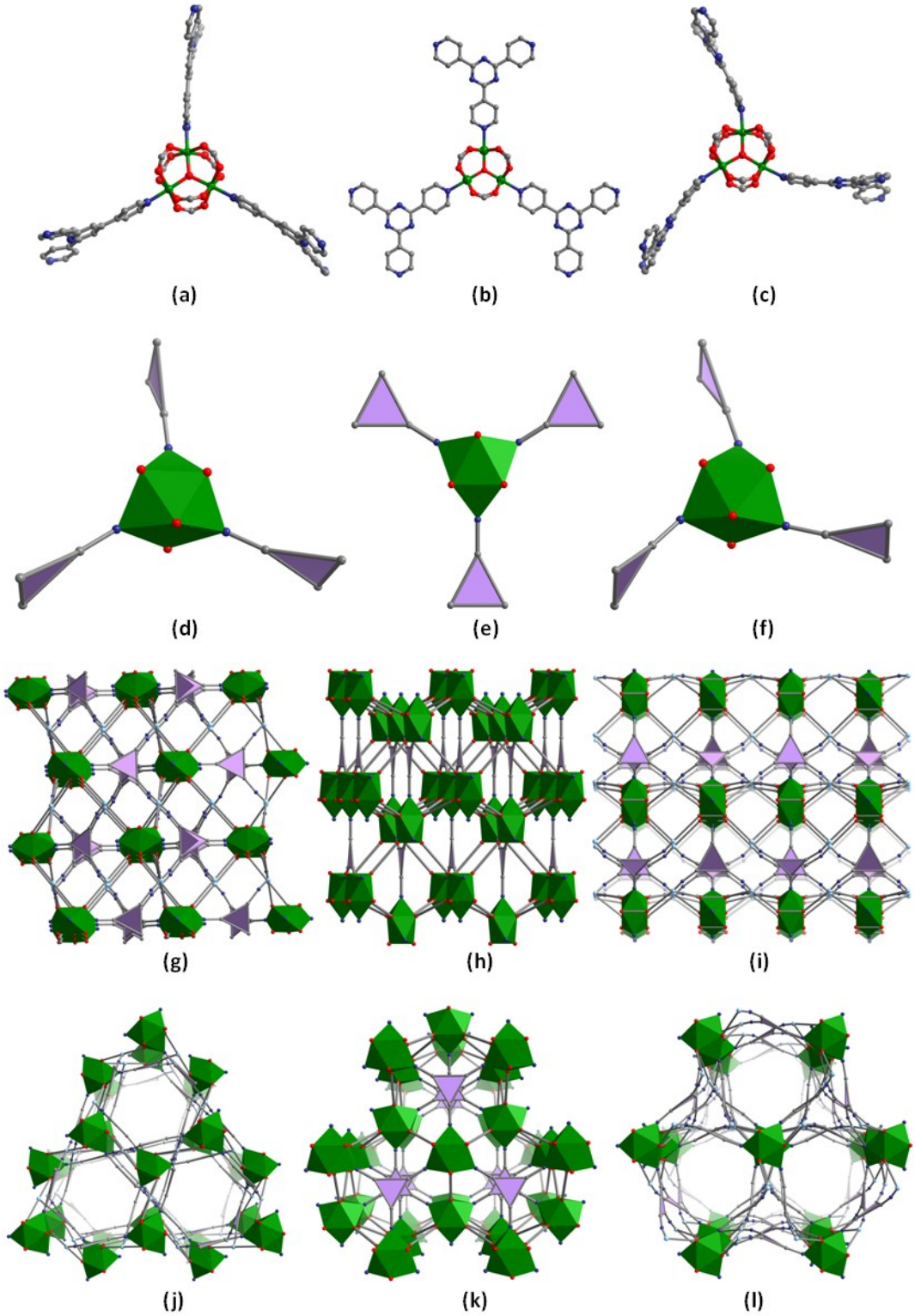

Figure S8. The linking modes between 9-c trinuclear cluster and tripyridine ligand and their resulting topological nets viewed along different directions: (a), (d), (g), (j) for SNNU-51-52; (b), (e), (h), (k) for pacs-MOFs; (c), (f), (i), (l) for SNUU-53-56.

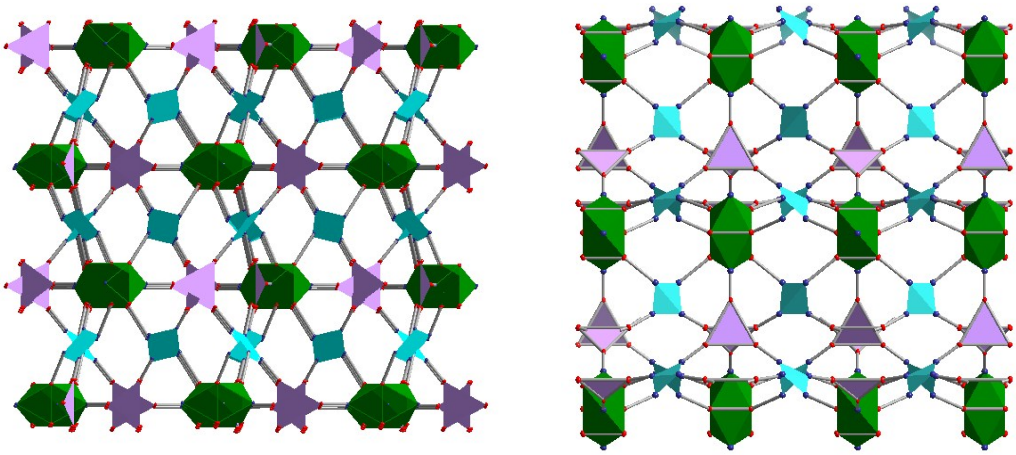

Figure S9. The 3,4,9-c topological nets with three polyhedral nodes for SNNU-51 (left) and SNNU-54 (right).

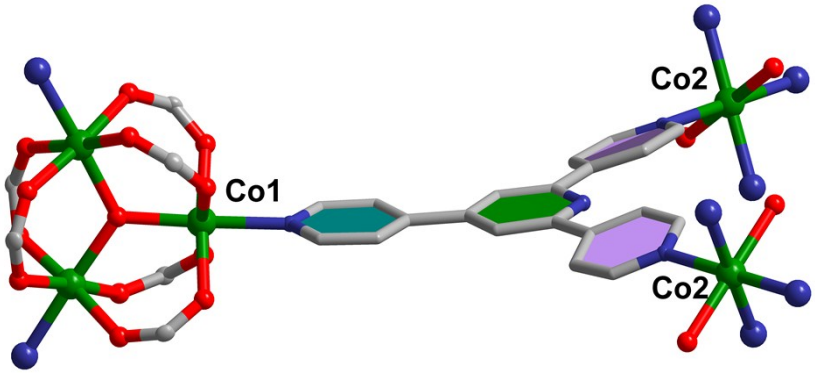

(a)

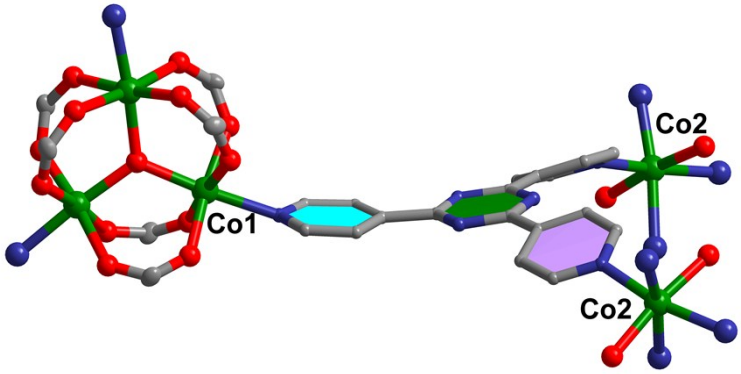

(b)

Figure S10. The configurations of TPP in SNNU-51 (a) and TPT in SNNU-54 (b).

Topological analysis results for SNNU-51-52:

Structure consists of 3D framework with V3TiSc3
Vertex symbols for selected sublattice

Sc1 Point symbol:{4^2.5^3.7}
Extended point symbol:[4.4.5.5.5(2).7(2)]

Ti1 Point symbol:{4^3.5^12.6^6.7^6.8^6.9^3}
Extended point
symbol:[4.4.4.5.5.5.5.5.5.5.5.5.5.5.6.6.6.6.6.6.7(2).7(2).7(2).7(2).7(2).7(2).8(2).8(2).8(2).8(2).8(2).8(2).
8(2).9(4).9(4).9(4)]

V1 Point symbol:{4.5^2}
Extended point symbol:[4.5.5]

Point symbol for net: {4.5^2}3{4^2.5^3.7}3{4^3.5^12.6^6.7^6.8^6.9^3}
3,4,9-c net with stoichiometry (3-c)3(4-c)3(9-c); 3-nodal net

Topological analysis results for SNNU-53-56:

Structure consists of 3D framework with V3TiSc3
Vertex symbols for selected sublattice

Sc1 Point symbol:{4^3.6^2.8}
Extended point symbol:[4.4.4(2).8(4).6(3).6(3)]

Ti1 Point symbol:{4^9.6^12.8^12.10^3}
Extended point
symbol:[4.4.4.4.4.4.4.4.6.6.6.6.6.6.6(2).6(2).6(2).6(2).6(2).6(2).8(2).8(2).8(2).8(2).8(2).8(2).8(2).8(2).
8(2).8(2).8(2).8(2).8(2).10(12).10(12).10(12)]

V1 Point symbol:{4.6^2}
Extended point symbol:[4.6.6]

Point symbol for net: {4.6^2}3{4^3.6^2.8}3{4^9.6^12.8^12.10^3}
3,4,9-c net with stoichiometry (3-c)3(4-c)3(9-c); 3-nodal net

Topological analysis results for pacs-MOFs:

Structure consists of 3D framework with TiSc
Vertex symbols for selected sublattice

Sc1 Point symbol:{4^21.6^15}
Extended point
symbol:[4.4.4.4.4.4.4.4.4.4.4.4(2).4(2).4(2).4(2).4(2).4(2).4(2).4(2).4(2).6(3).6(3).6(3).6(15).6(15).
6(15).6(15).6(15).6(15).6(4).6(4).6(4).6(4).6(4).6(4)]

Ti1 Point symbol:{4^3}
Extended point symbol:[4(2).4(2).4(2)]

Point symbol for net: {4^21.6^15}{4^3}
3,9-c net with stoichiometry (3-c)(9-c); 2-nodal net

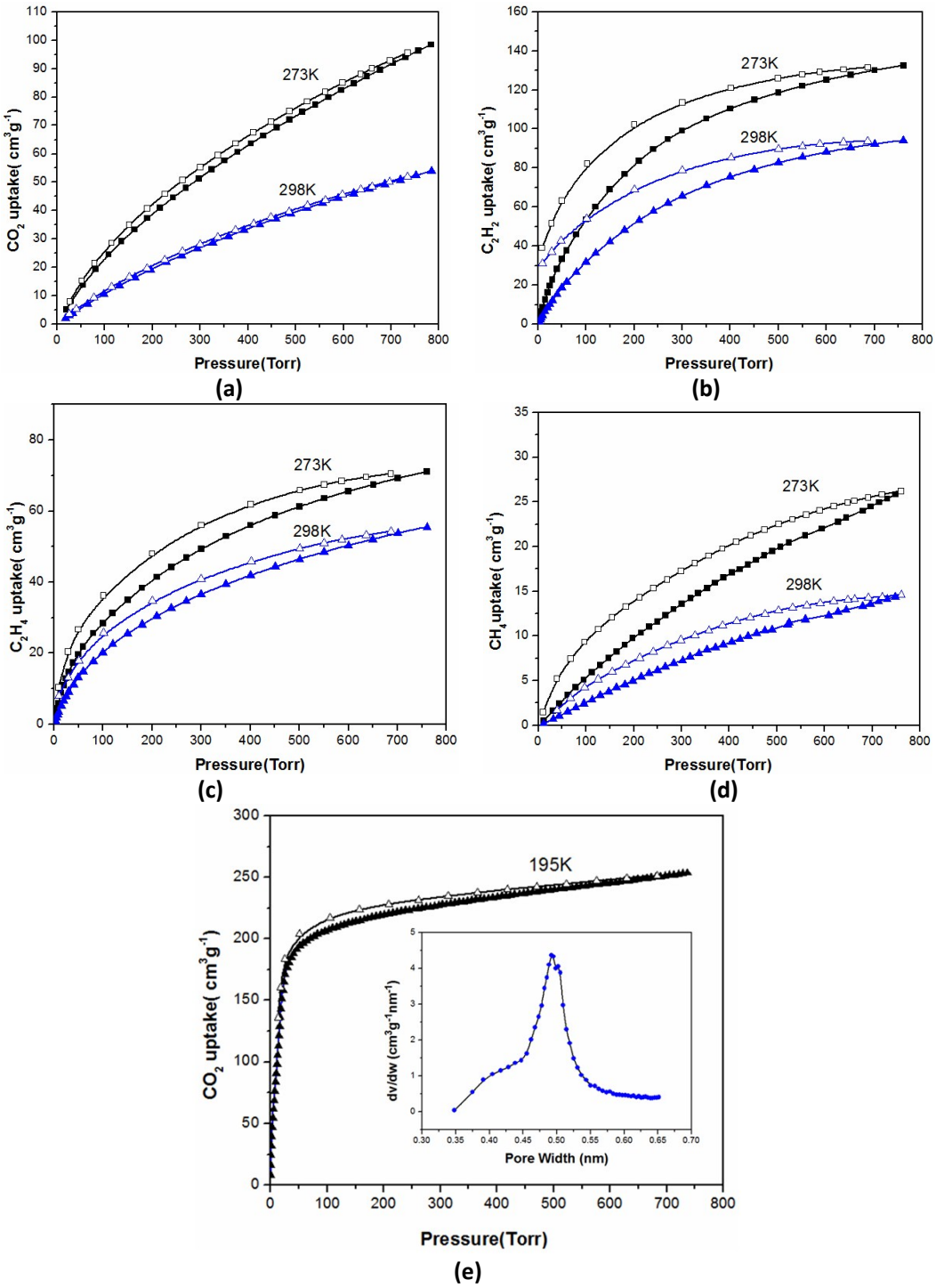

Figure S11. CO_2, CH_4, C_2H_4 and C_2H_2 adsorption and desorption isotherms at 273 and 298 K, and CO_2 uptake at 195 K for SNNU-51.

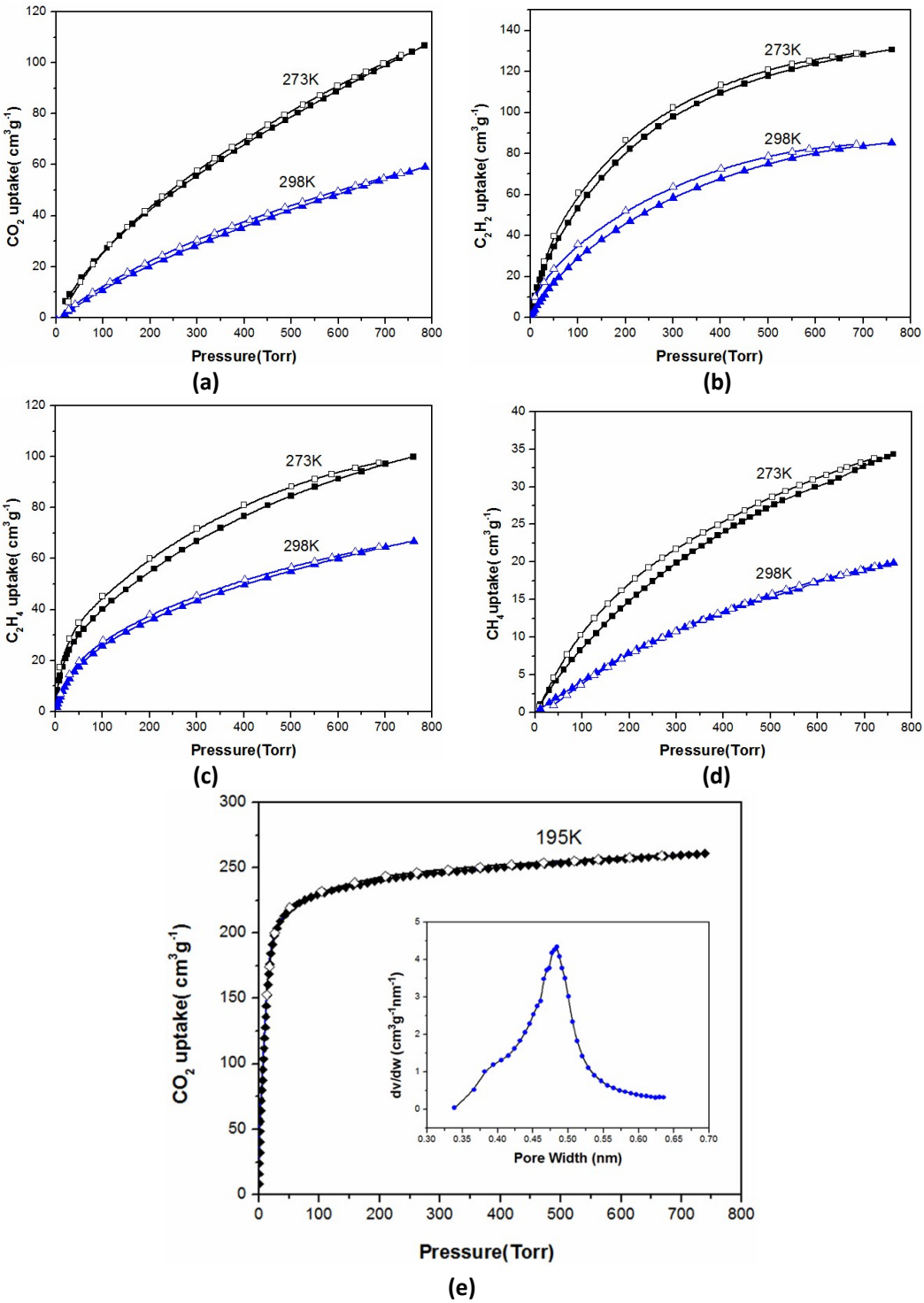

Figure S12. CO_2, CH_4, C_2H_4 and C_2H_2 adsorption and desorption isotherms at 273 and 298 K, and CO_2 uptake at 195 K for SNNU-52.

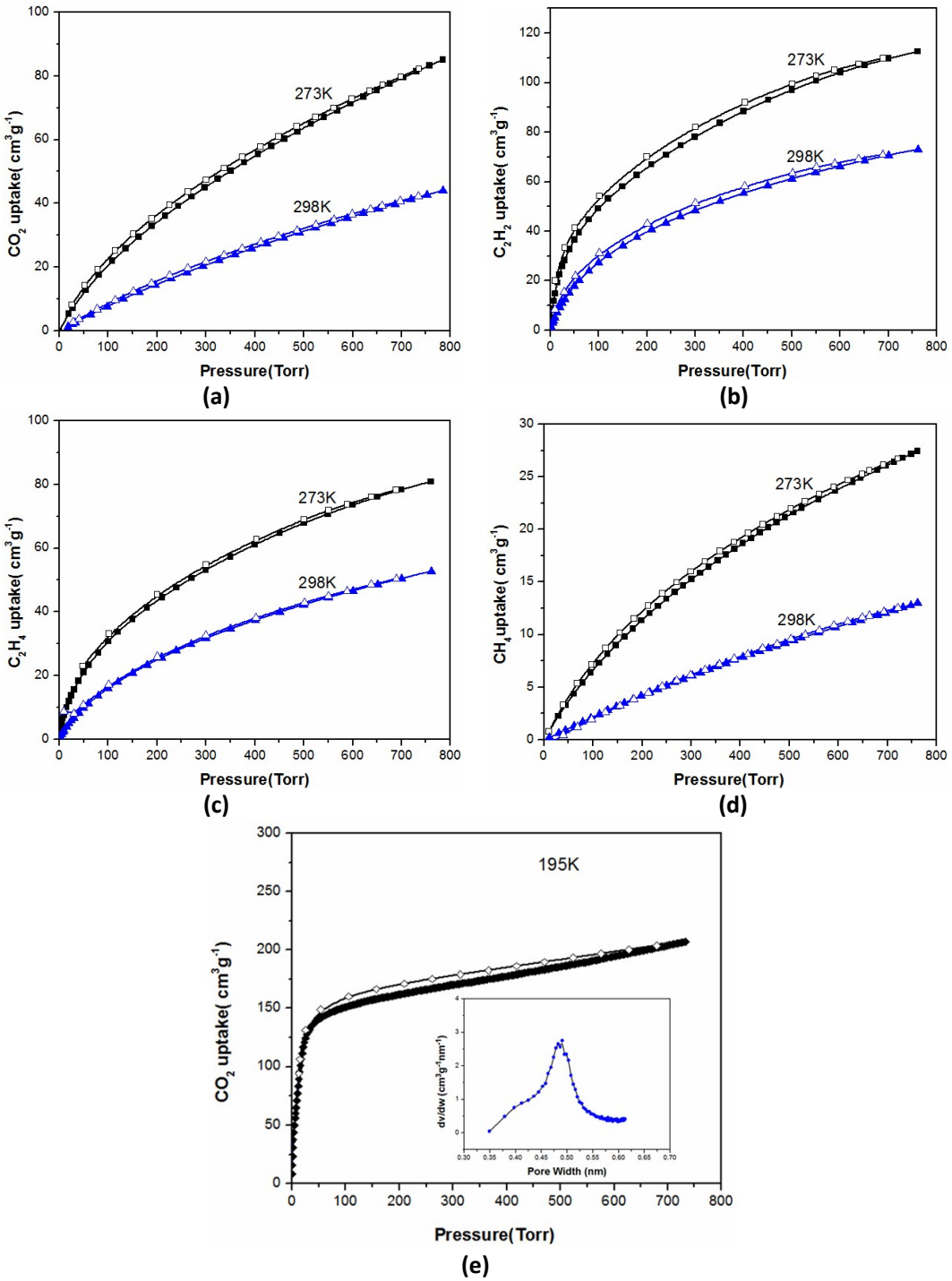

Figure S13. CO_2, CH_4, C_2H_4 and C_2H_2 adsorption and desorption isotherms at 273 and 298 K, and CO_2 uptake at 195 K for SNNU-53.

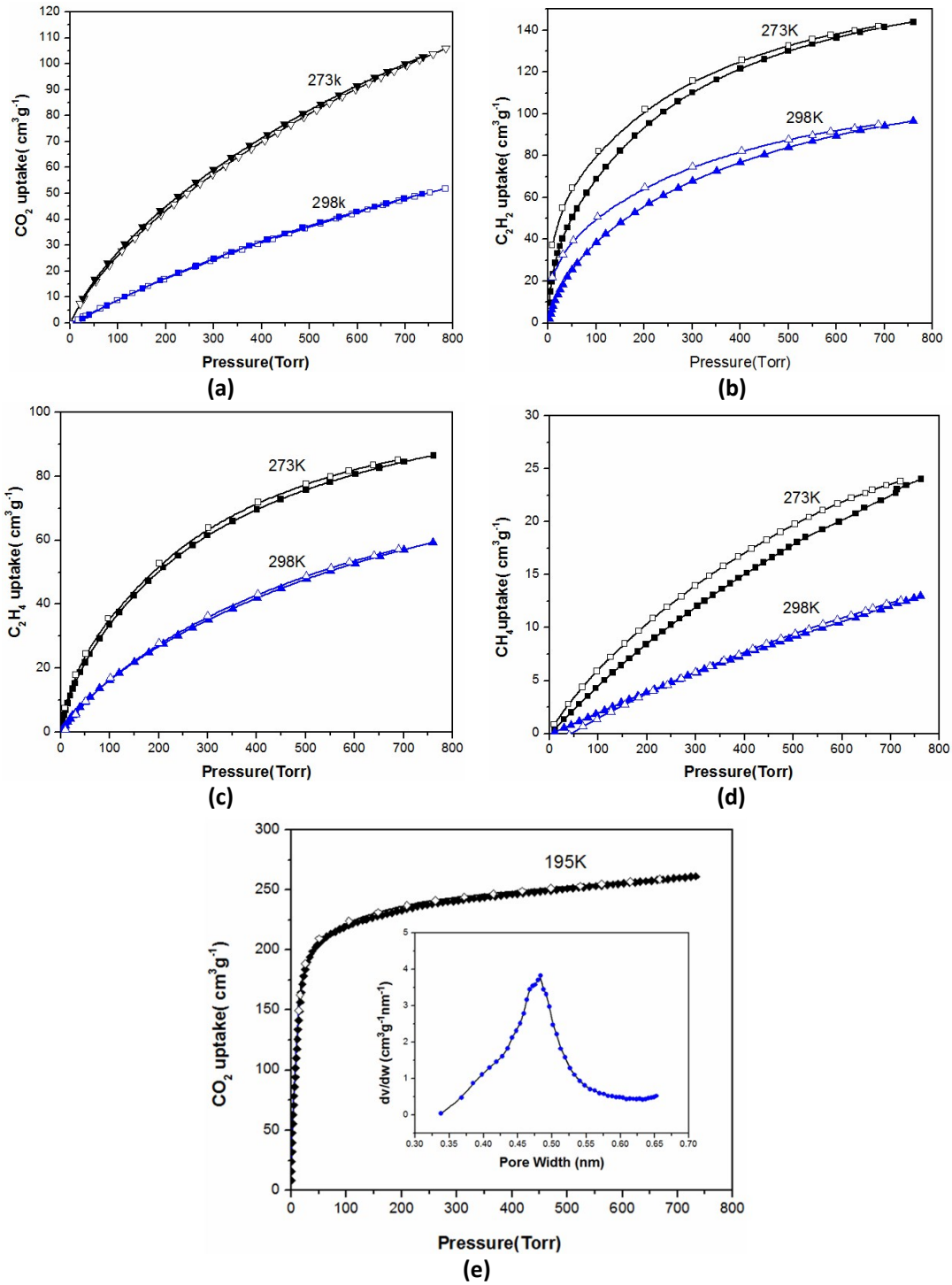

Figure S14. CO_2, CH_4, C_2H_4 and C_2H_2 adsorption and desorption isotherms at 273 and 298 K, and CO_2 uptake at 195 K for SNNU-54.

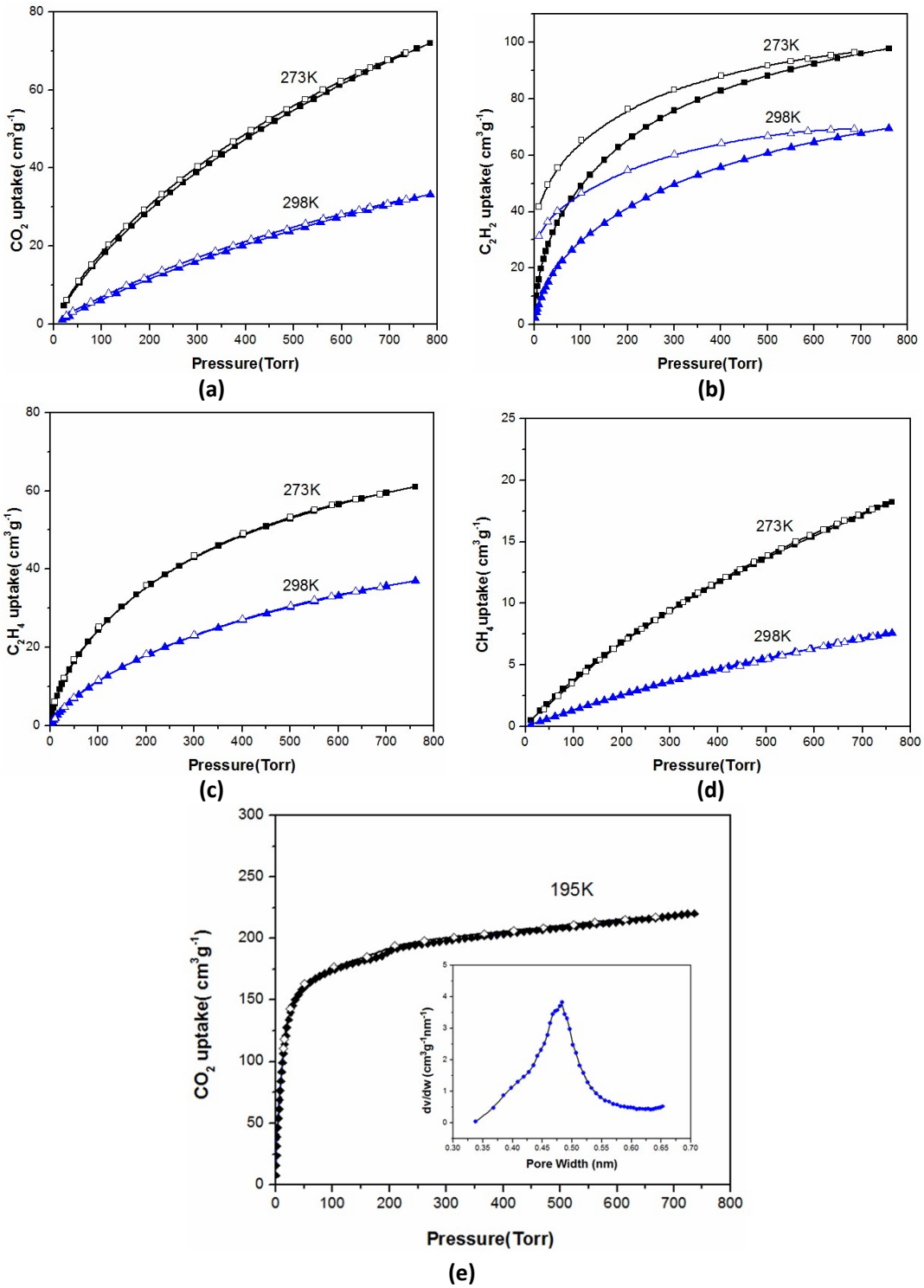

Figure S15. CO_2, CH_4, C_2H_4 and C_2H_2 adsorption and desorption isotherms at 273 and 298 K, and CO_2 uptake at 195 K for SNNU-55.

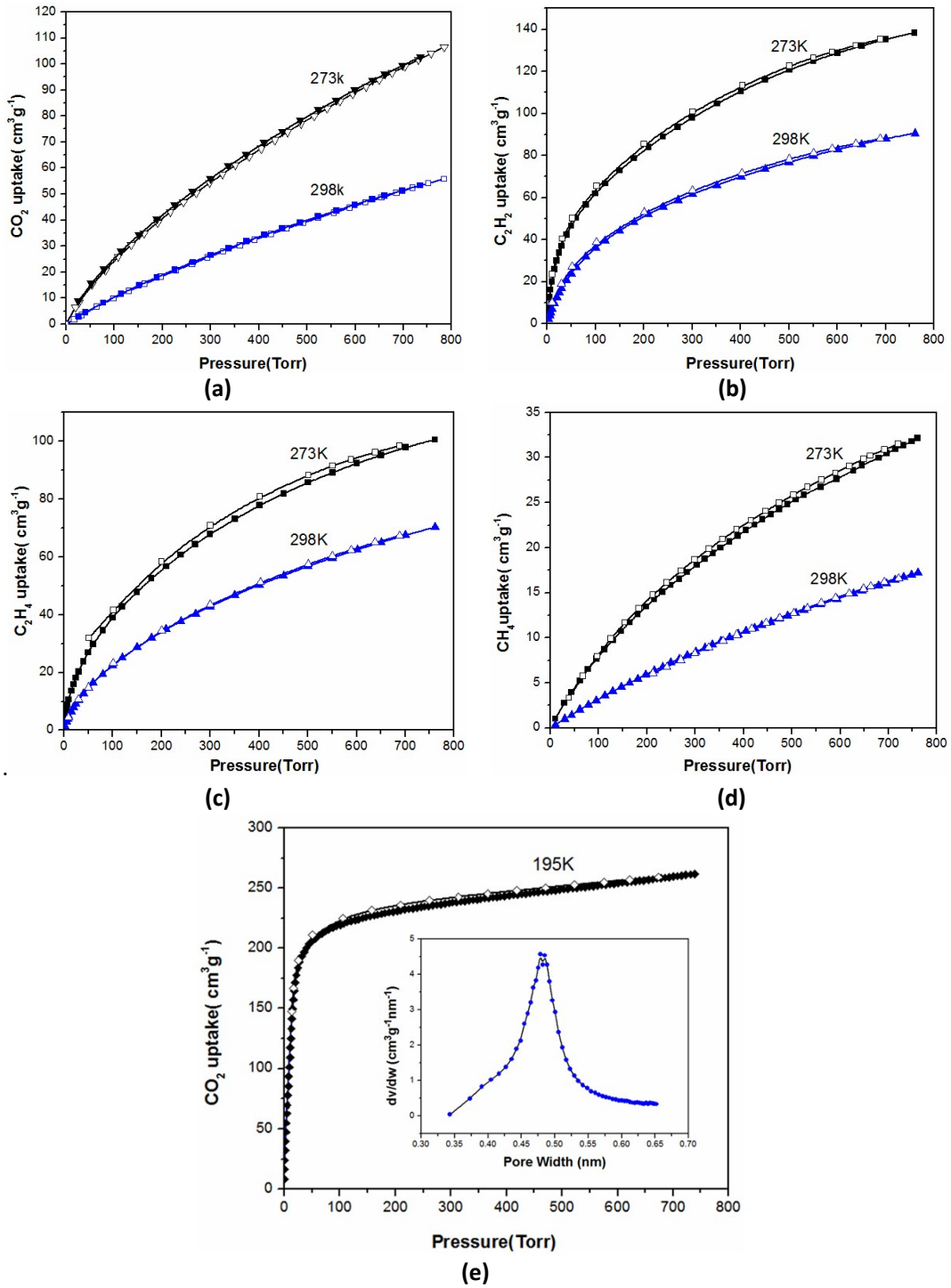

Figure S16. CO_2, CH_4, C_2H_4 and C_2H_2 adsorption and desorption isotherms at 273 and 298 K, and CO_2 uptake at 195 K for SNNU-56.

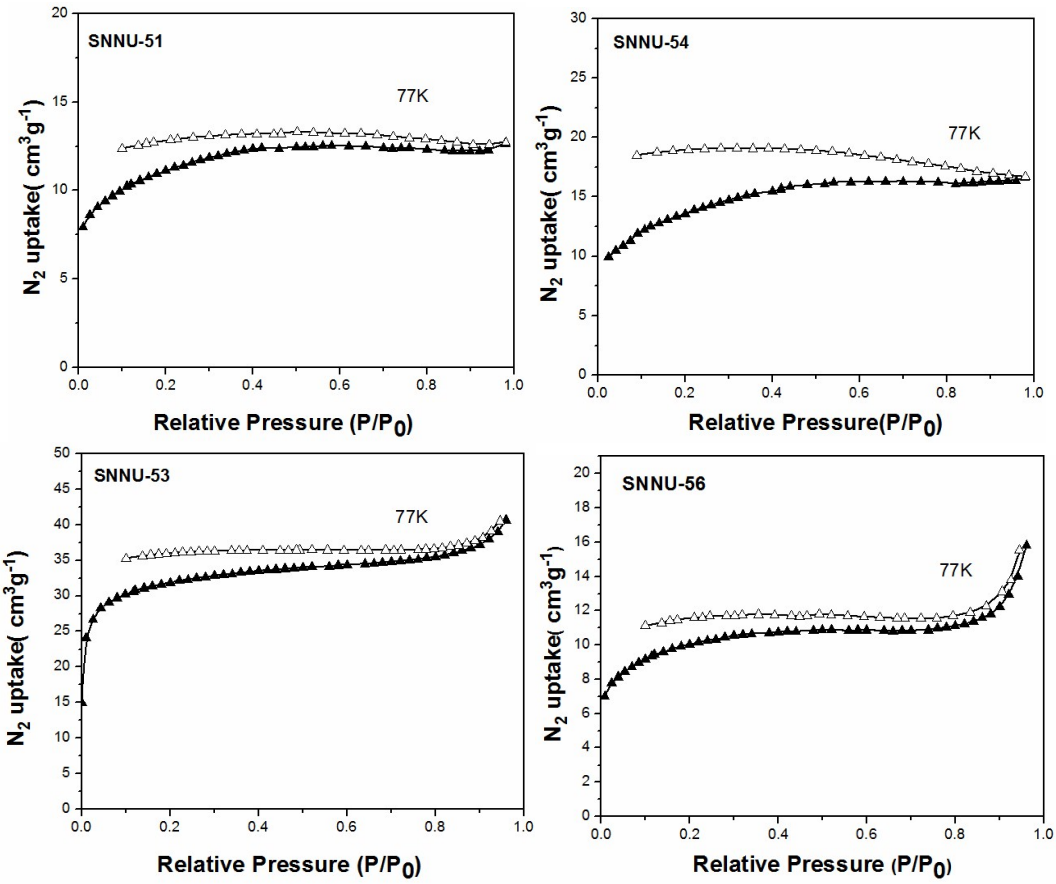

Figure S17. N_2 adsorption and desorption isotherms for SNNU-51, -53, -54, and -56 at 77 K.

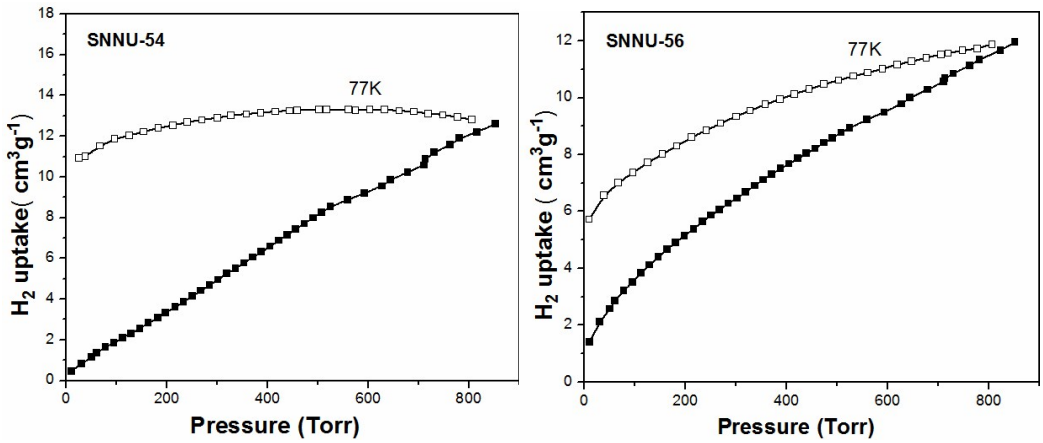

Figure S18. H_2 adsorption and desorption isotherms for SNNU-54 and -56 at 77 K.

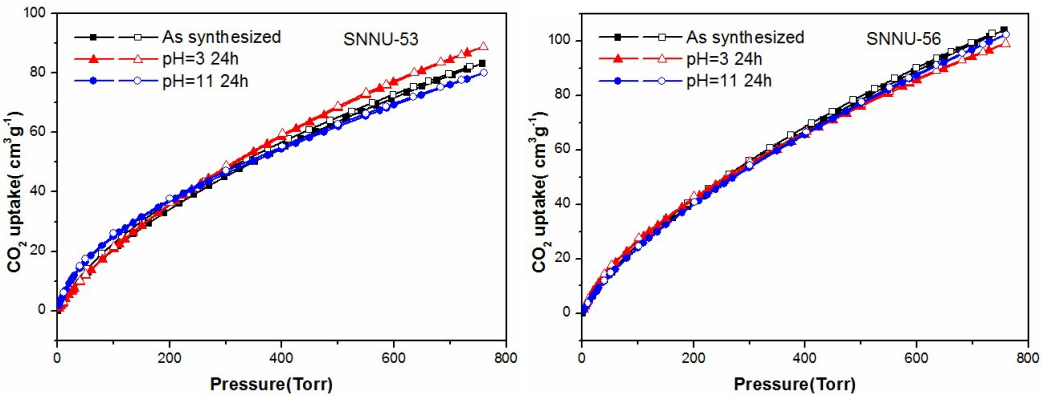

Figure S19. CO_2 adsorption and desorption isotherms at 273 K for SNNU-53 and -56 after treated in water at pH = 3 and 11.

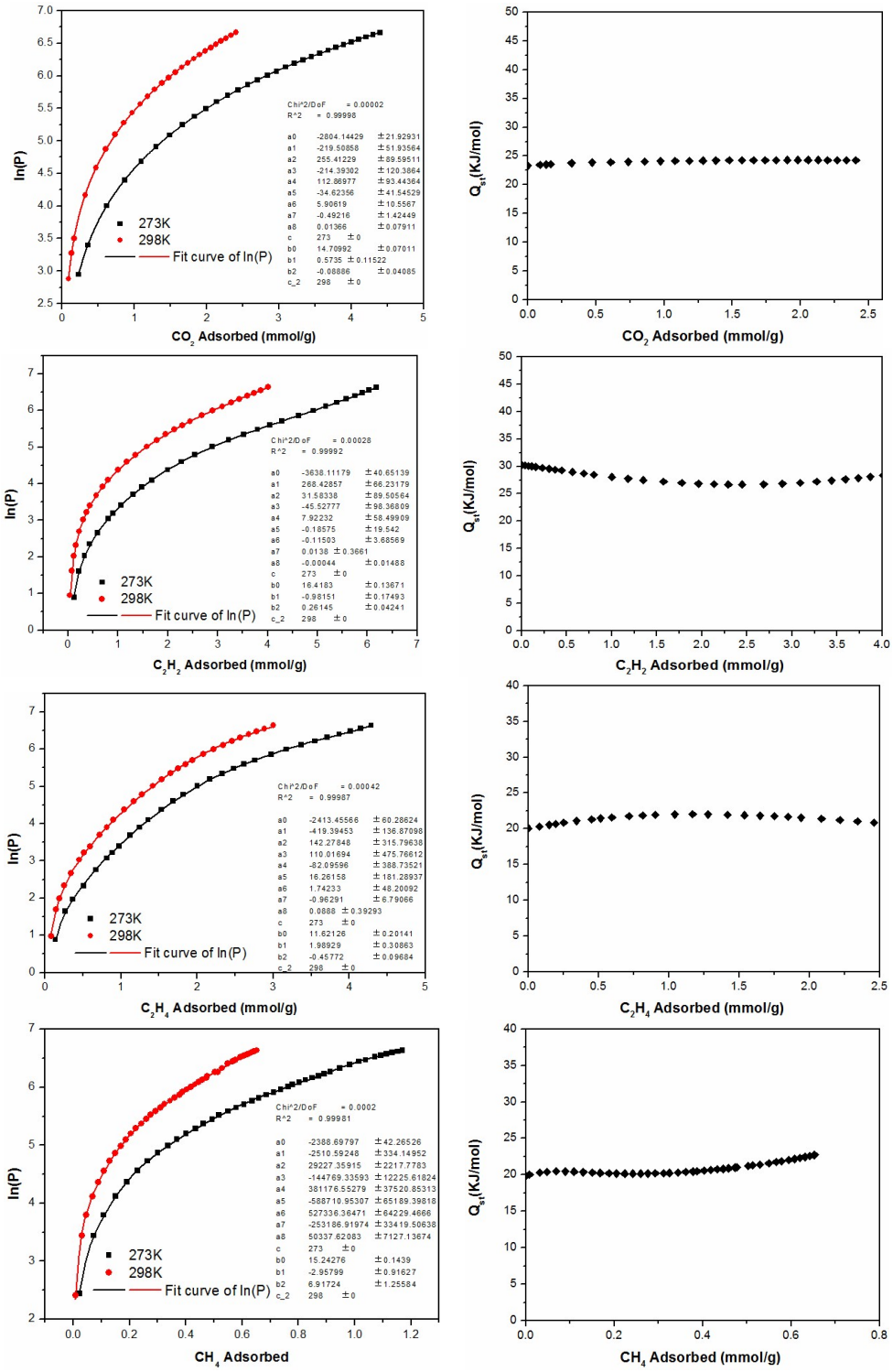

Figure S20. Fitted gas adsorption isotherms of SNNU-51 measured at 273 and 298 K, and their corresponding isosteric heats of adsorption (Q_{st}).

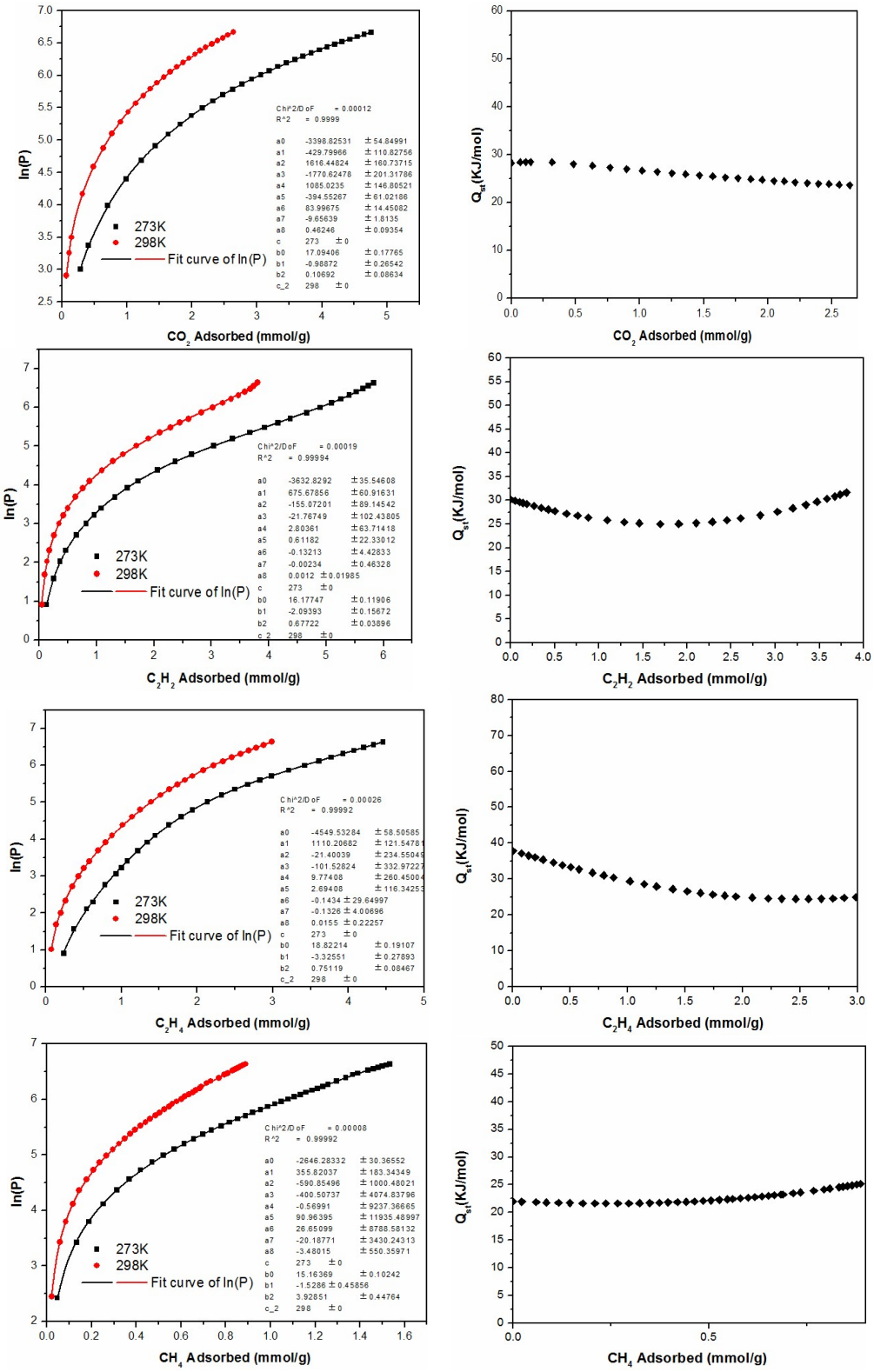

Figure S21. Fitted gas adsorption isotherms of SNNU-52 measured at 273 and 298 K, and their corresponding isosteric heats of adsorption (Q_{st}).

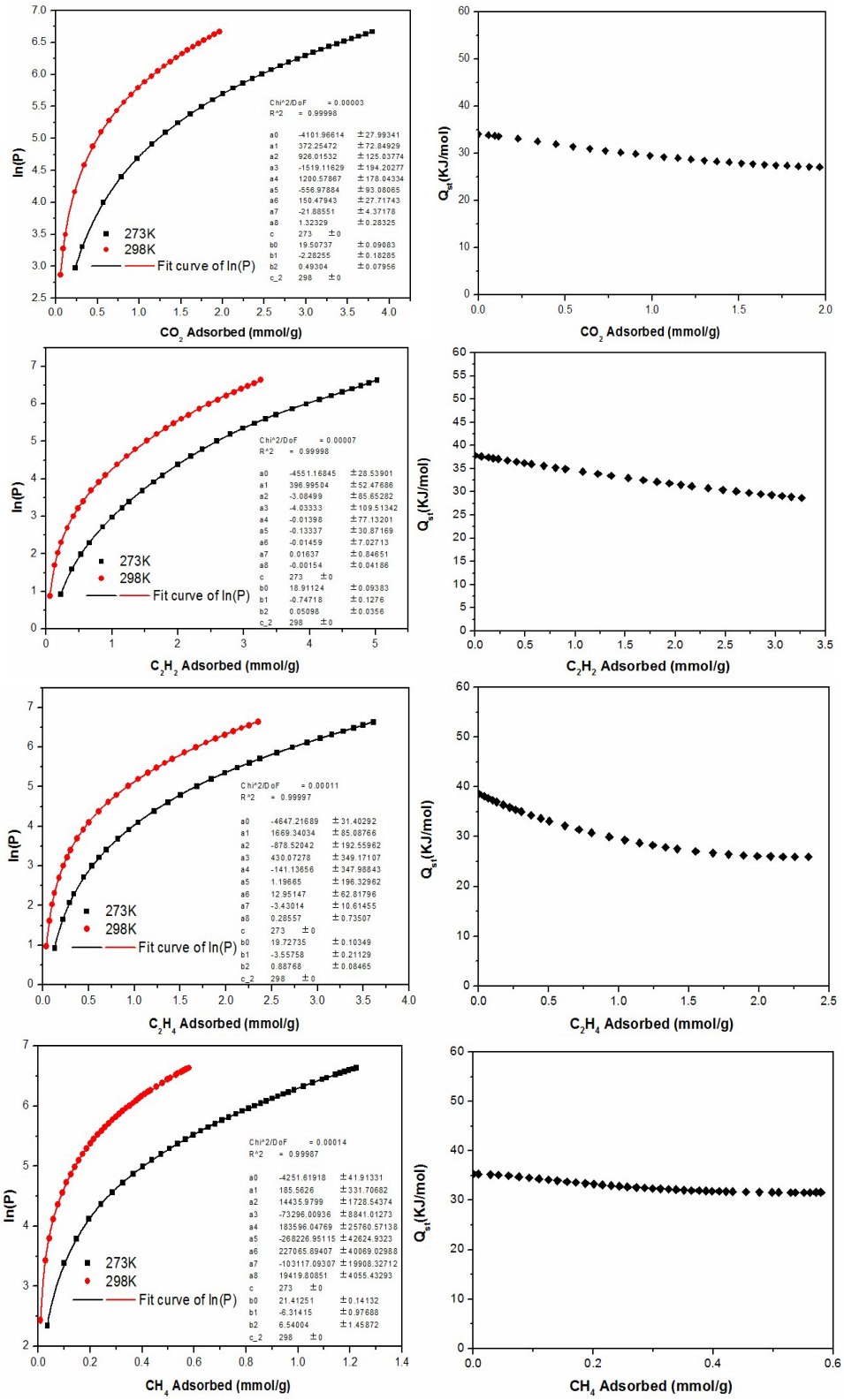

Figure S22. Fitted gas adsorption isotherms of SNNU-53 measured at 273 and 298 K, and their corresponding isosteric heats of adsorption (Q_{st}).

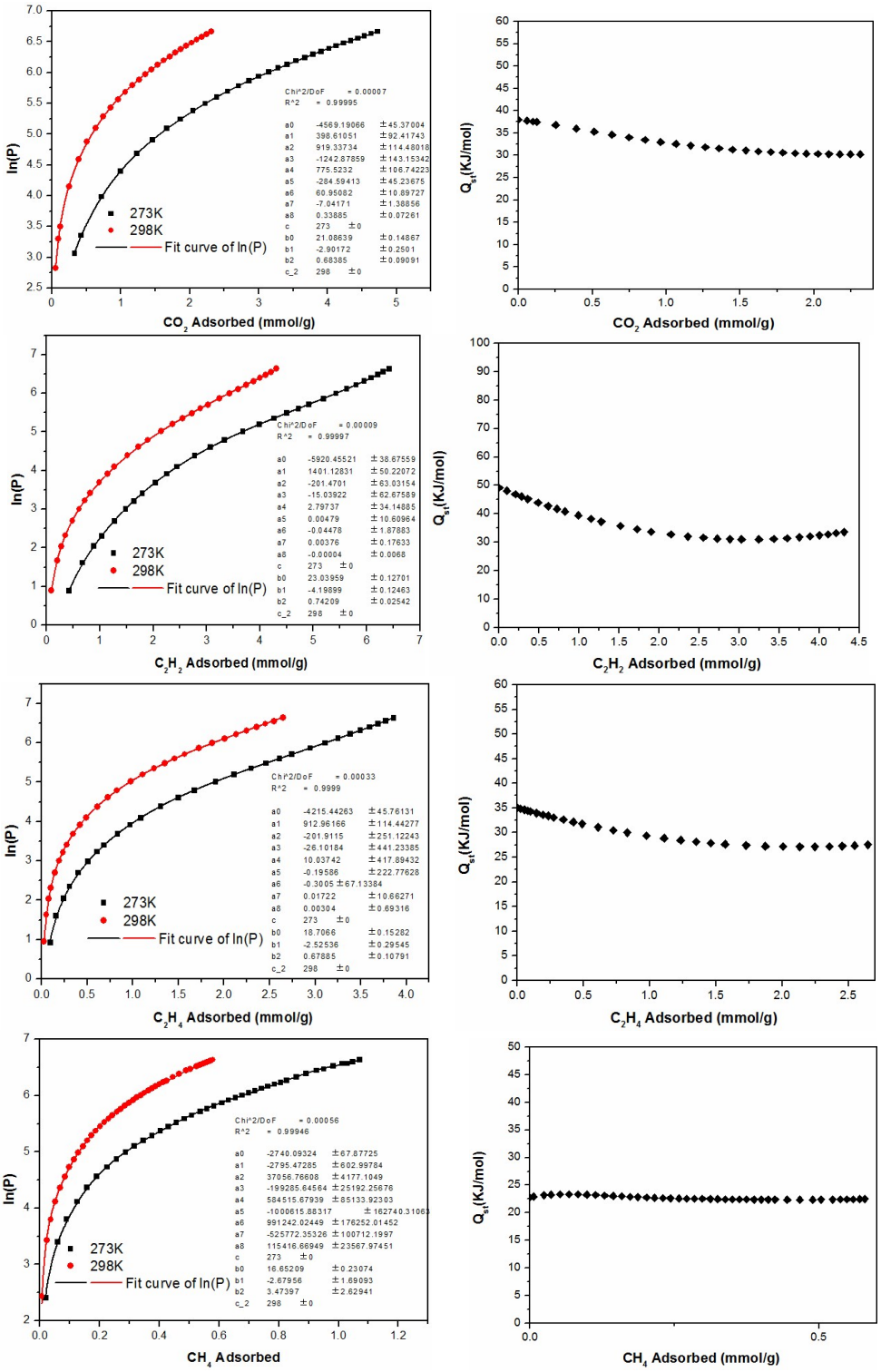

Figure S23. Fitted gas adsorption isotherms of SNNU-54 measured at 273 and 298 K, and their corresponding isosteric heats of adsorption (Q_{st}).

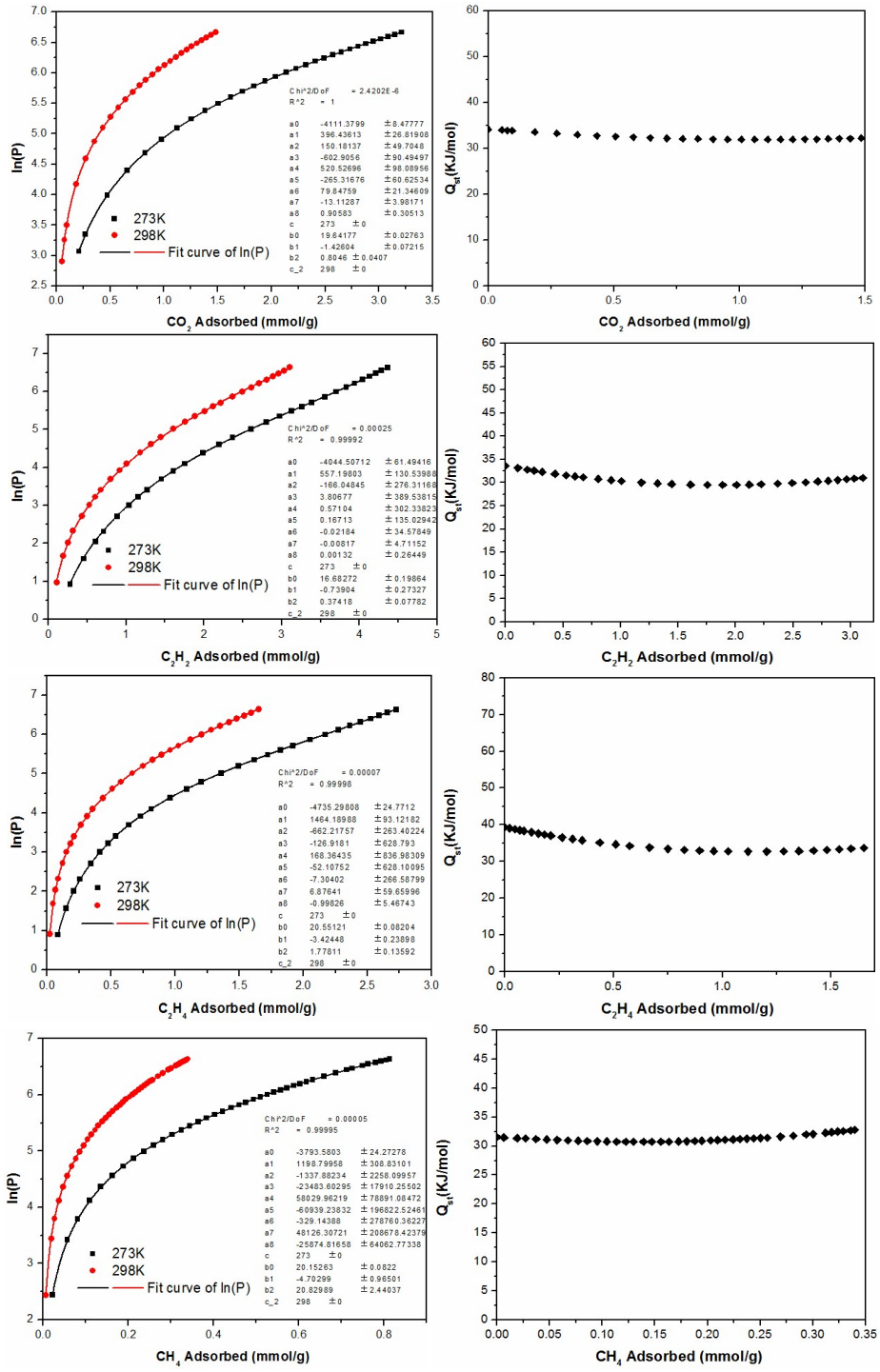

Figure S24. Fitted gas adsorption isotherms of SNNU-55 measured at 273 and 298 K, and their corresponding isosteric heats of adsorption (Q_{st}).

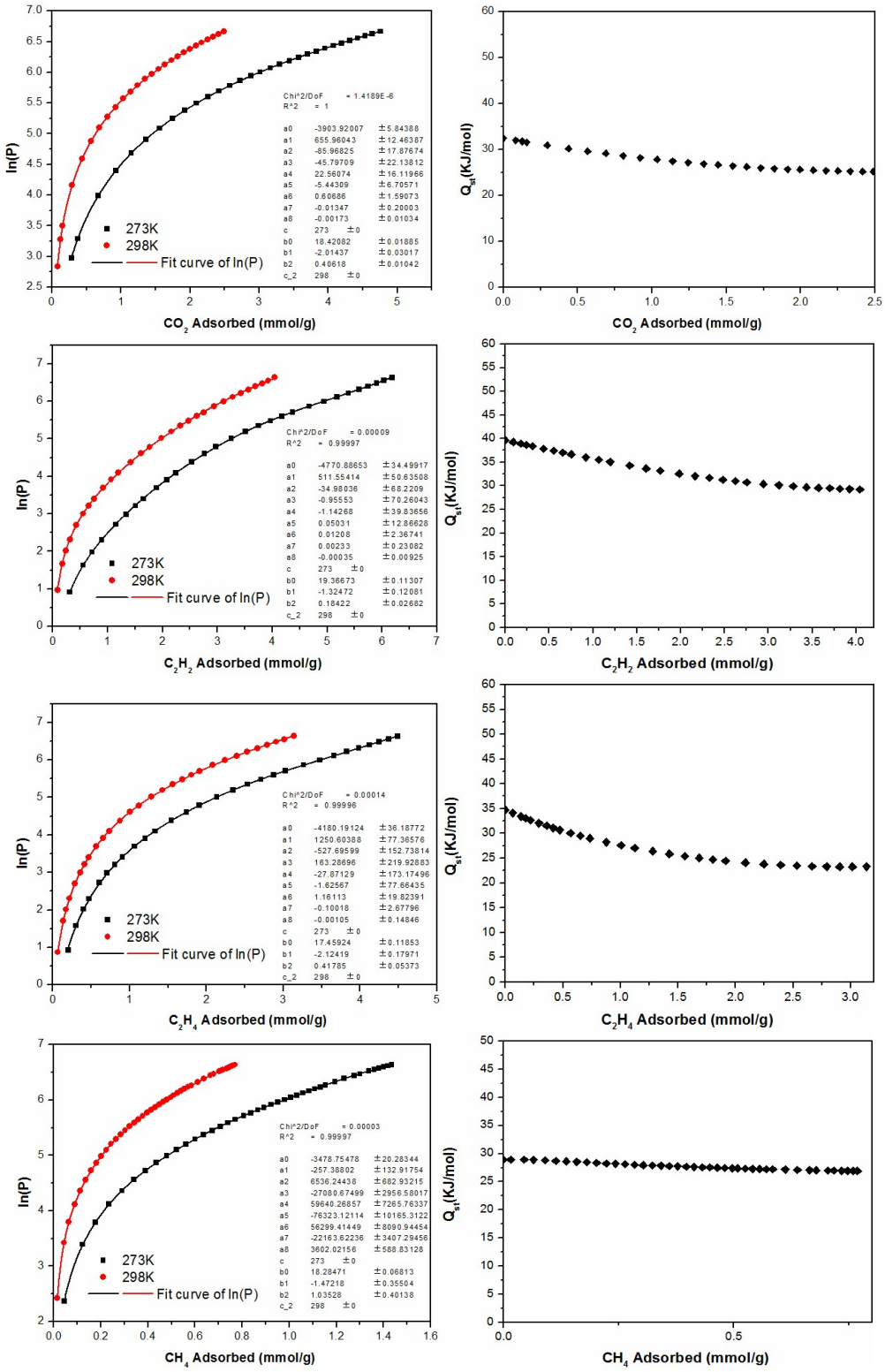

Figure S25. Fitted gas adsorption isotherms of SNNU-56 measured at 273 and 298 K, and their corresponding isosteric heats of adsorption (Q_{st}).

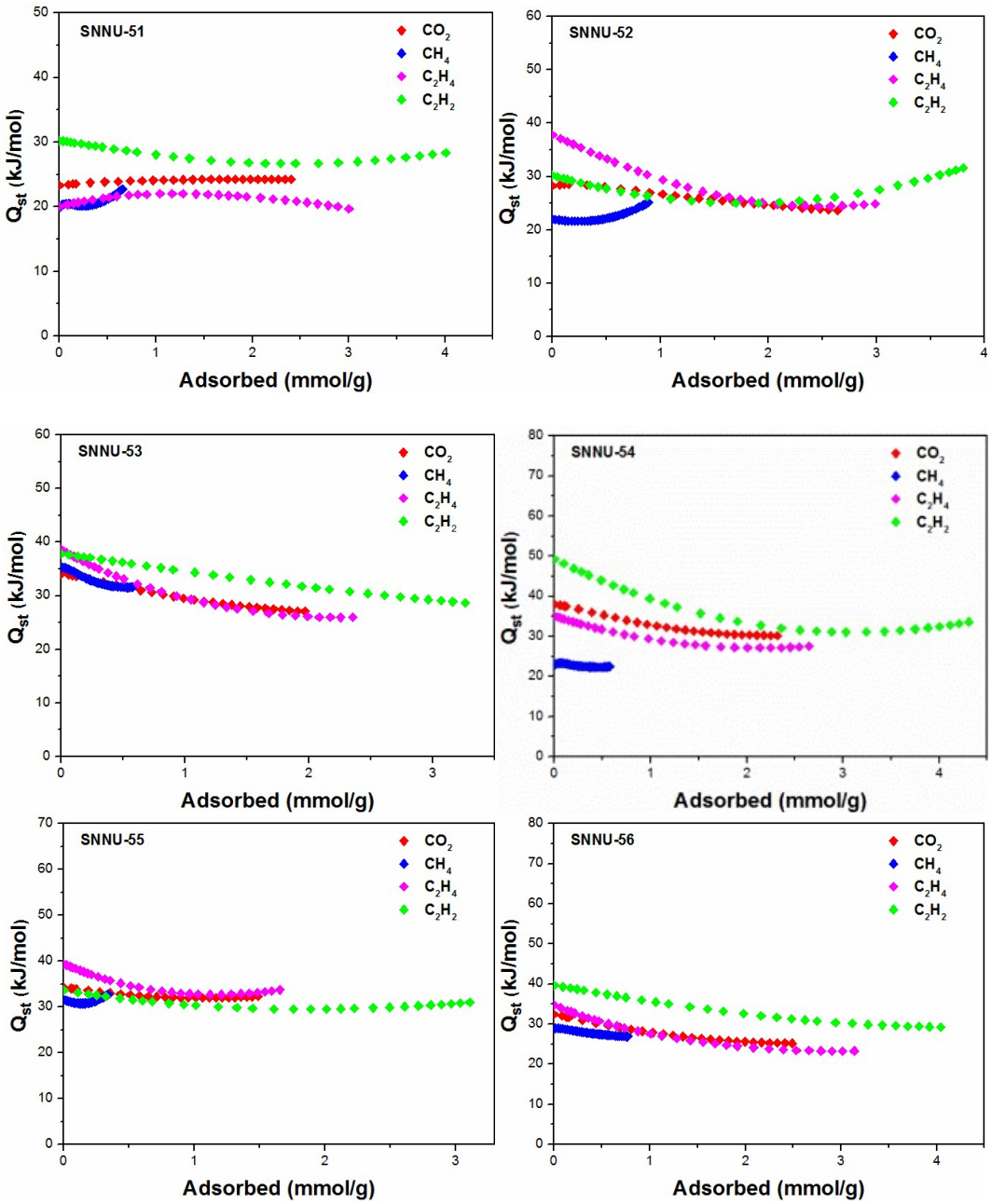

Figure S26. The comparisons of isosteric heats of adsorption (Q_{st}) with low loading for SNNU-51-56.

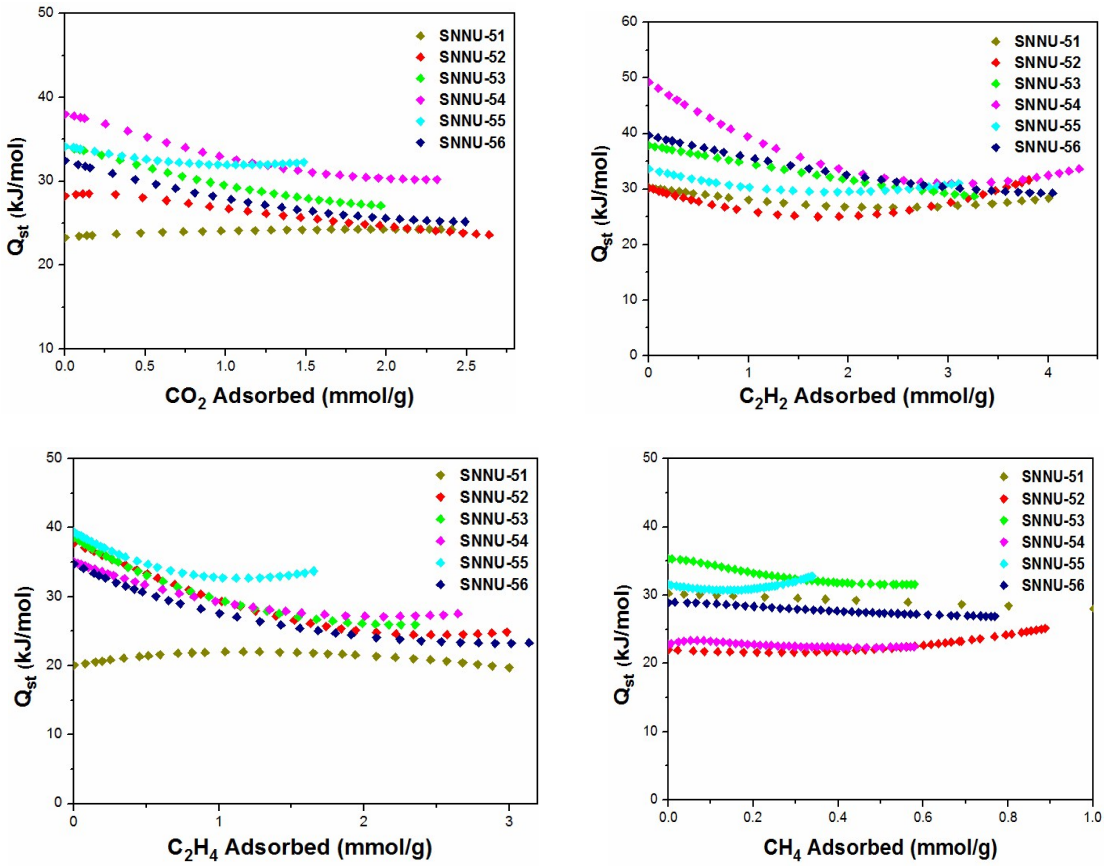

Figure S27. The comparisons of isosteric heats of adsorption (Q_{st}) with low loading for all compounds.

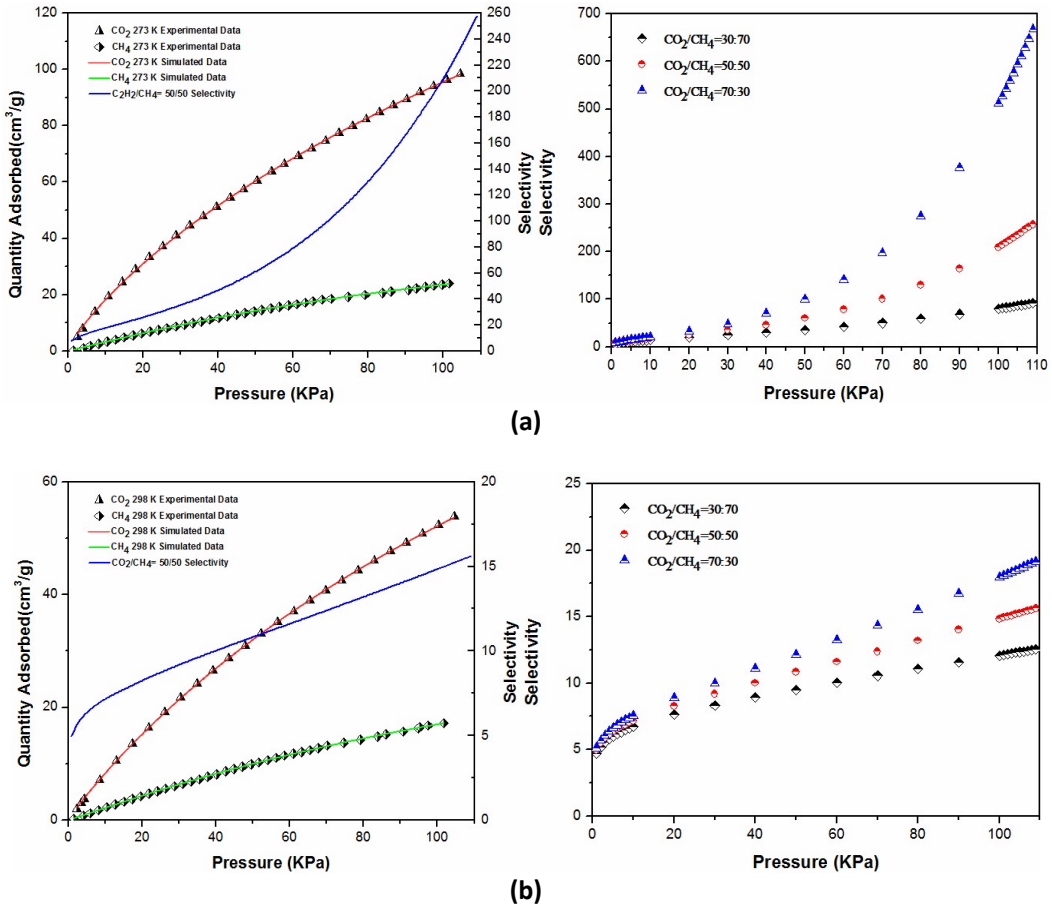

Figure S28. The selectivity predicted by IAST of SNNU-51 for binary mixture CO_2/CH_4 at 273 K (a) and 298 K (b).

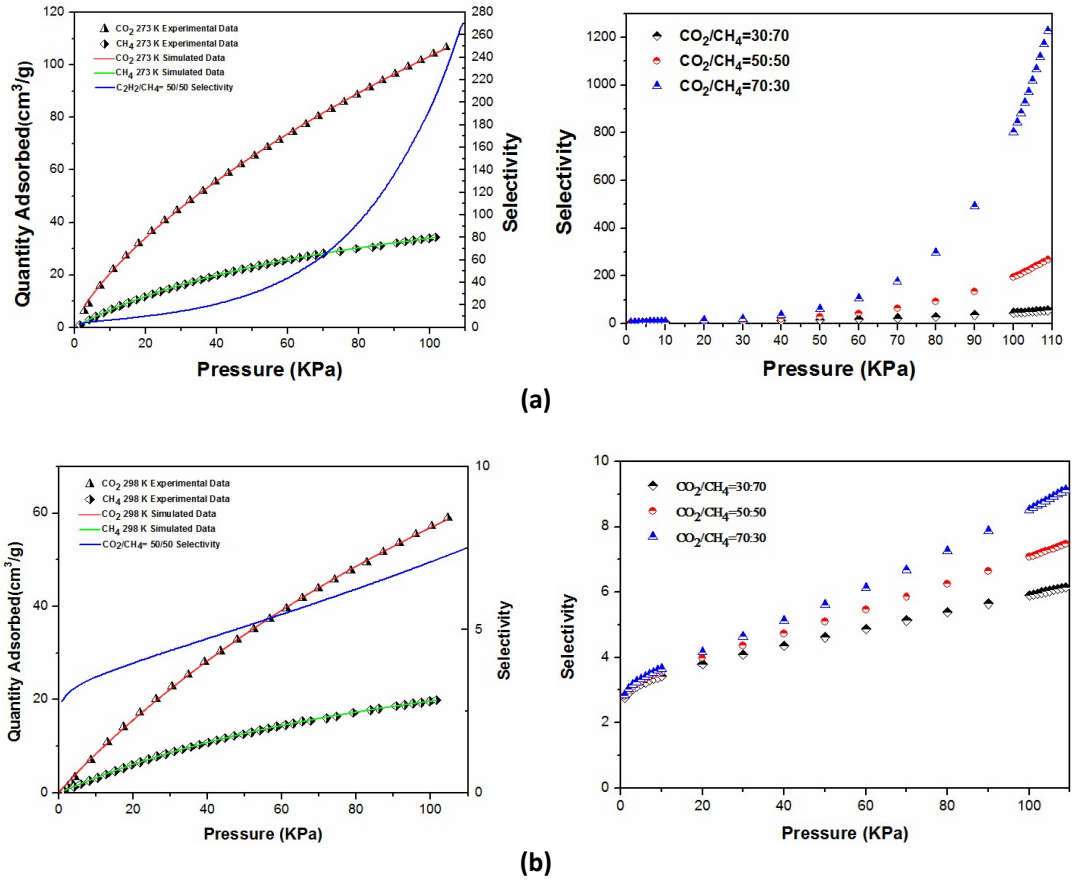

Figure S29. The selectivity predicted by IAST of SNNU-52 for binary mixture CO_2/CH_4 at 273 K (a) and 298 K (b).

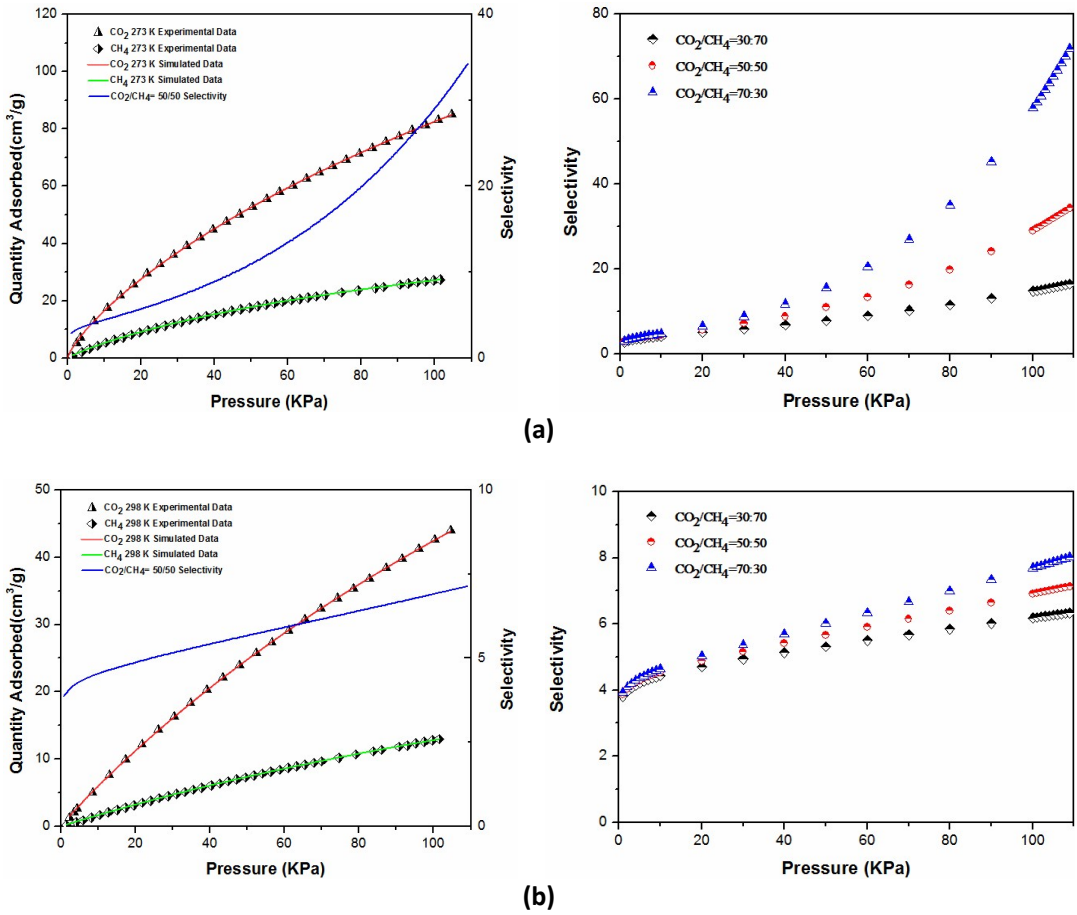

Figure S30. The selectivity predicted by IAST of SNNU-53 for binary mixture CO_2/CH_4 at 273 K (a) and 298 K (b).

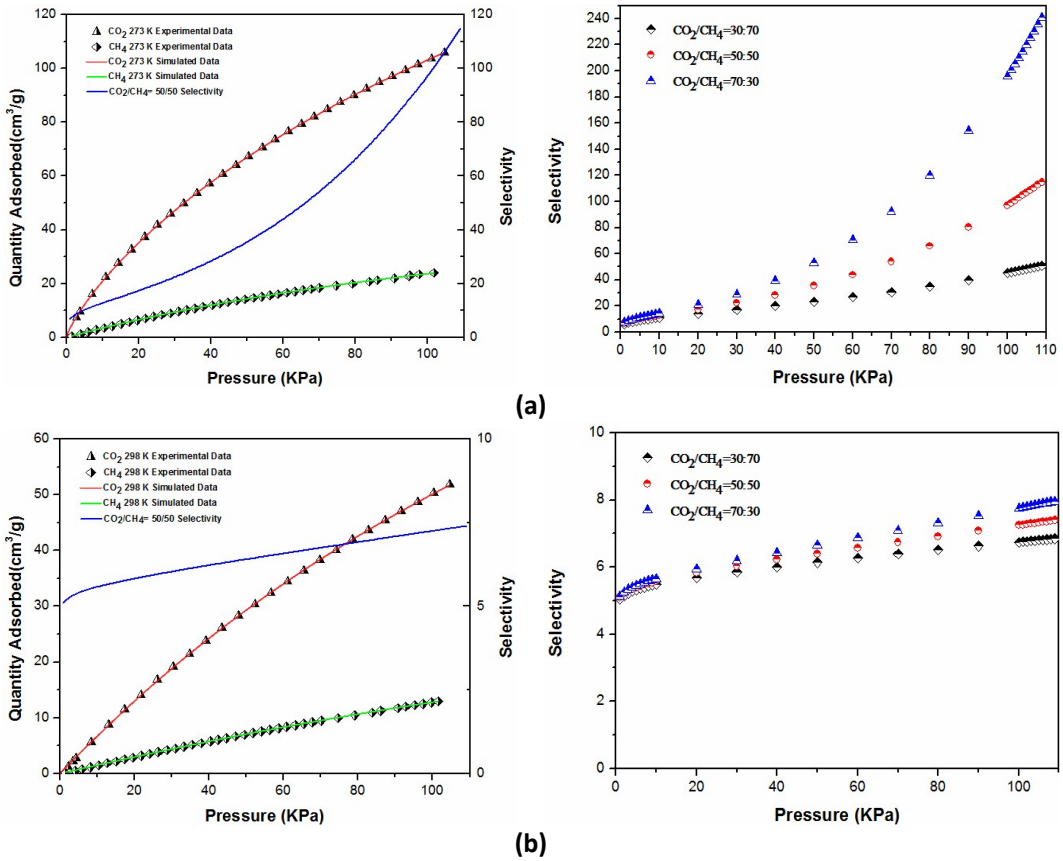

Figure S31. The selectivity predicted by IAST of SNNU-54 for binary mixture CO_2/CH_4 at 273 K (a) and 298 K (b).

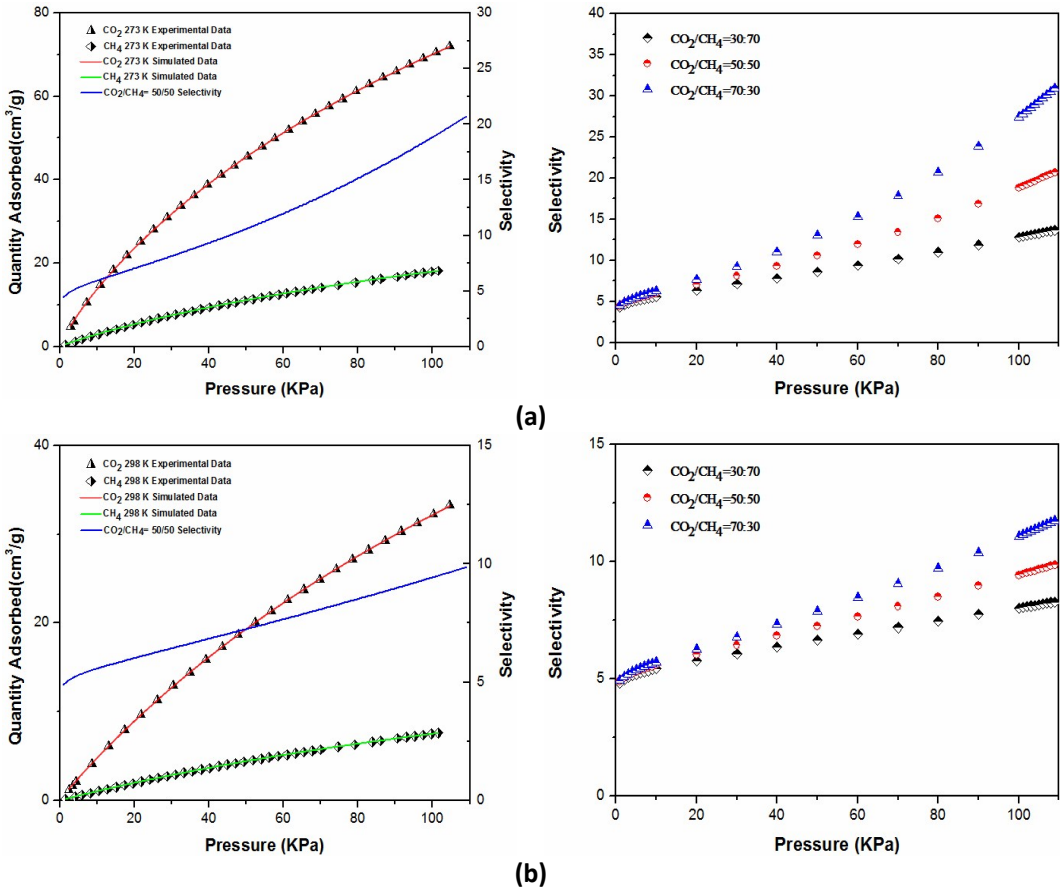

Figure S32. The selectivity predicted by IAST of SNNU-55 for binary mixture CO_2/CH_4 at 273 K (a) and 298 K (b).

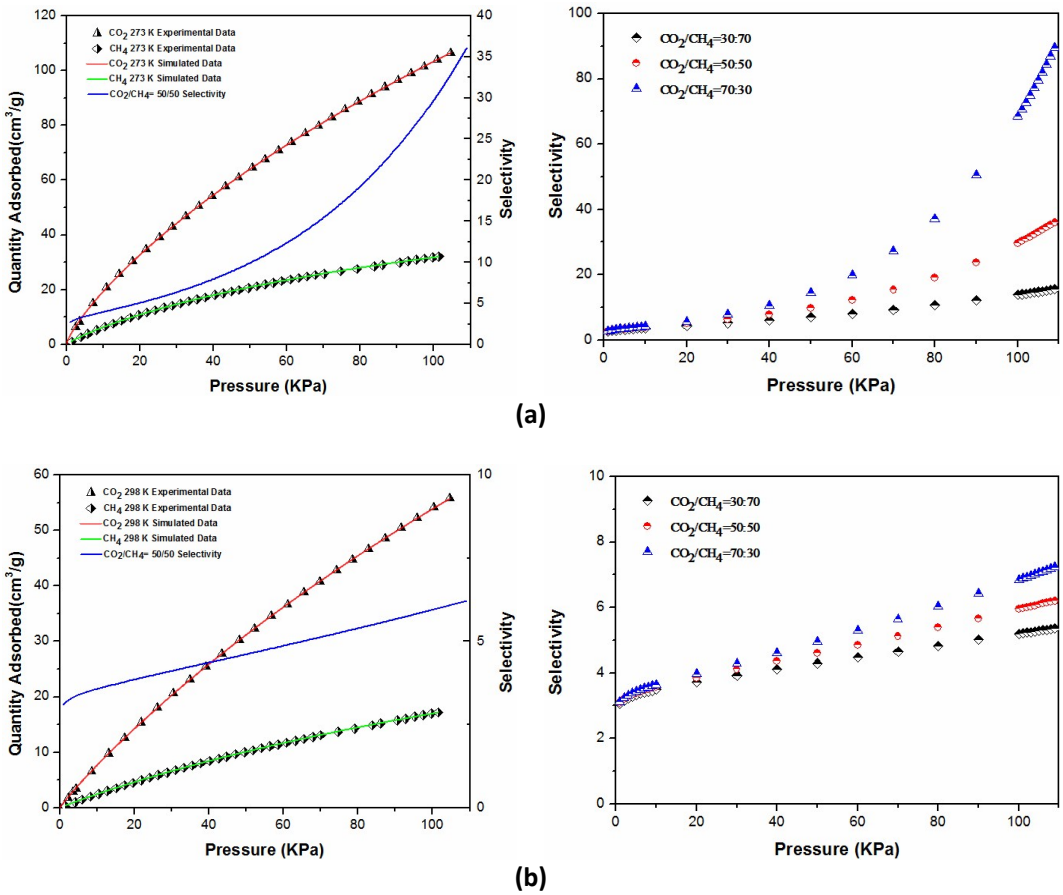

Figure S33. The selectivity predicted by IAST of SNNU-56 for binary mixture CO_2/CH_4 at 273 K (a) and 298 K (b).

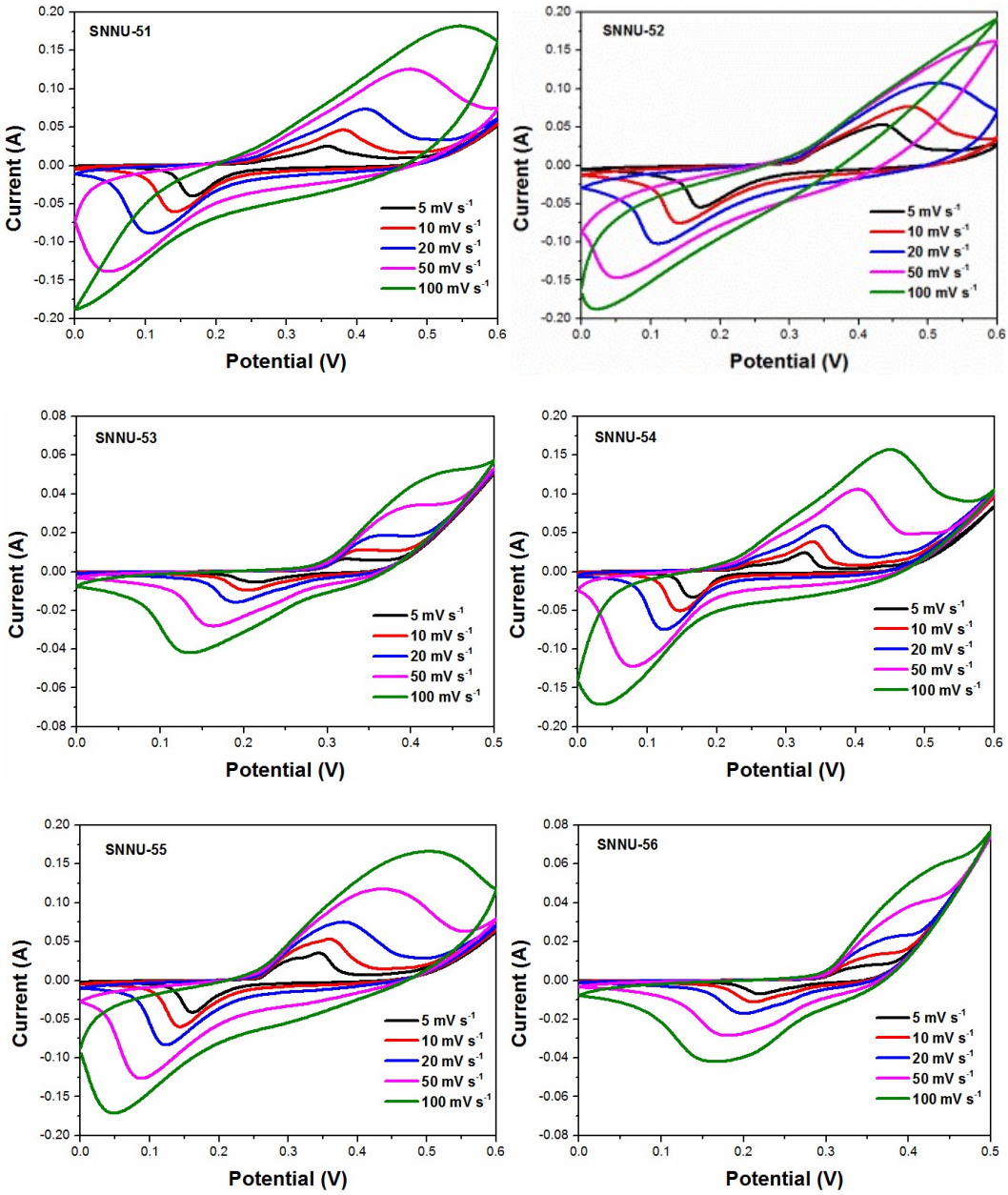

Figure S34. CV curves of SNNU-51-56 MOF electrodes at different scan rates.

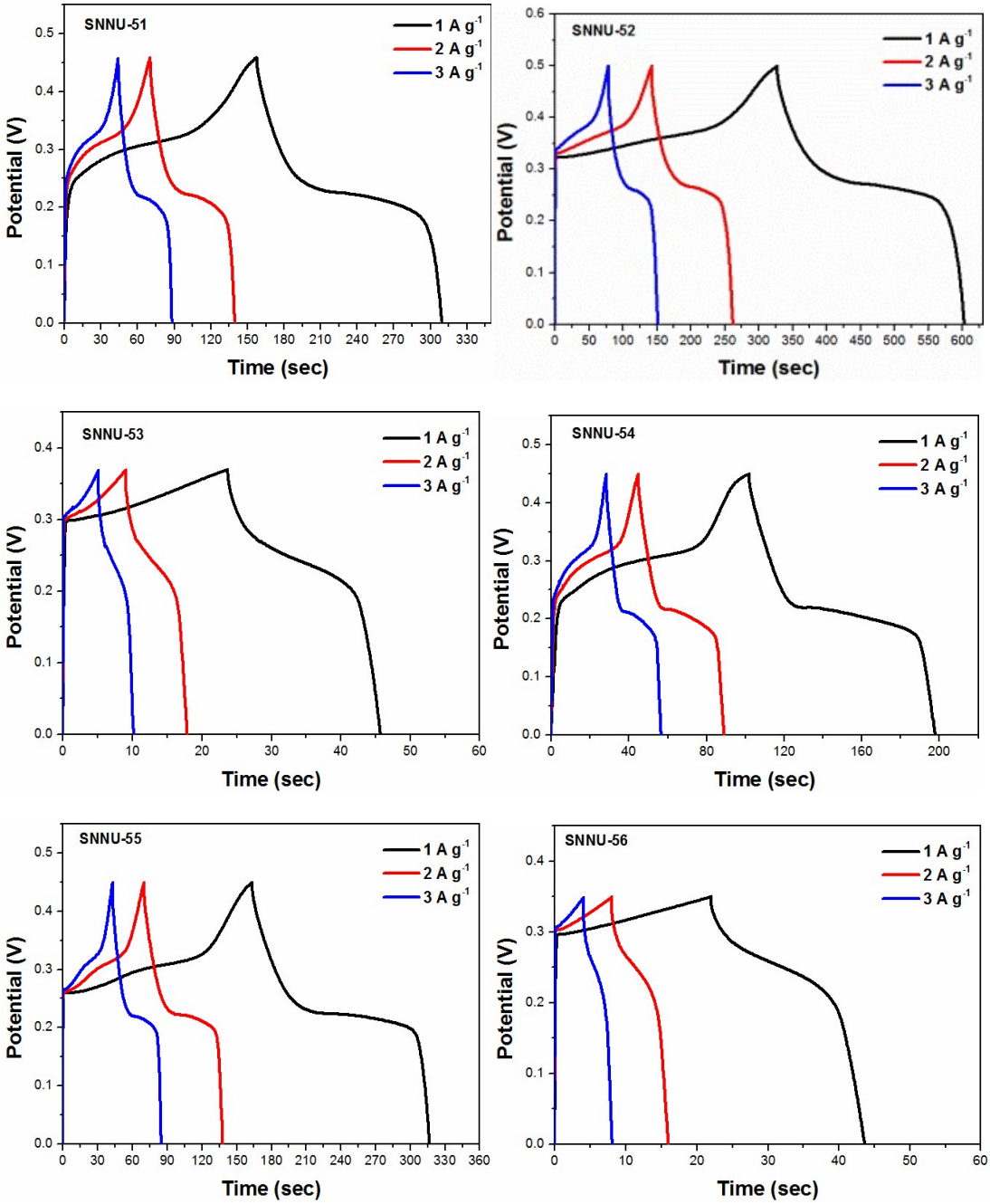

Figure S35. Galvanostatic charge-discharge curves of SUUN-51-56 at different current densities.

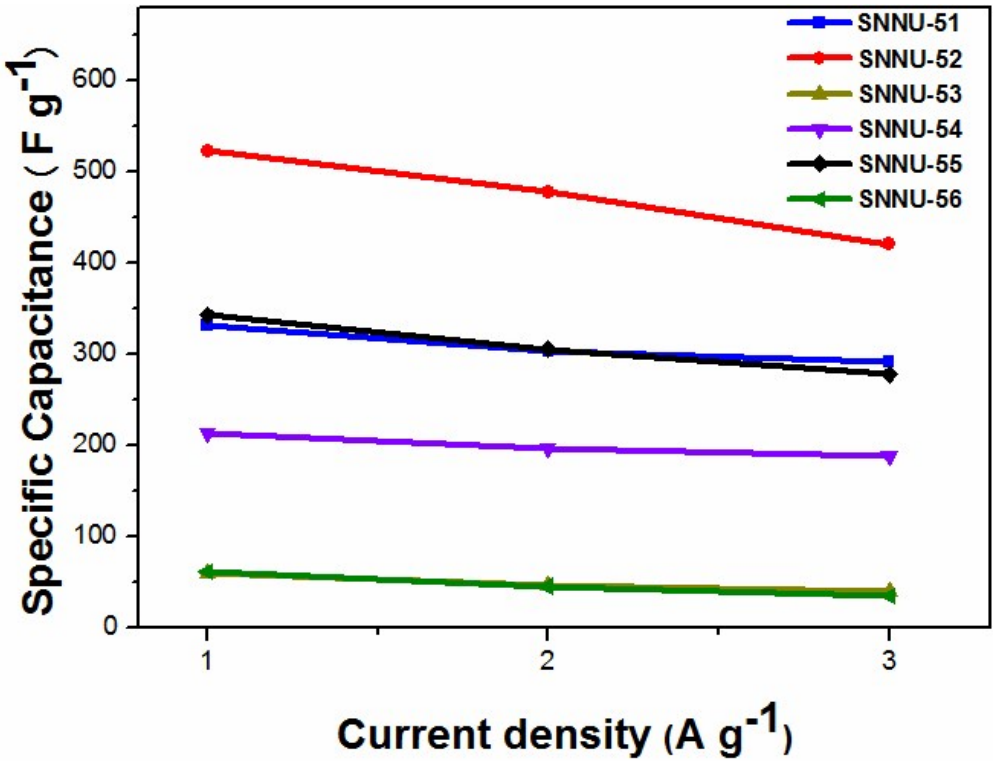

Figure S36. Specific capacity of six MOFs at various current densities.

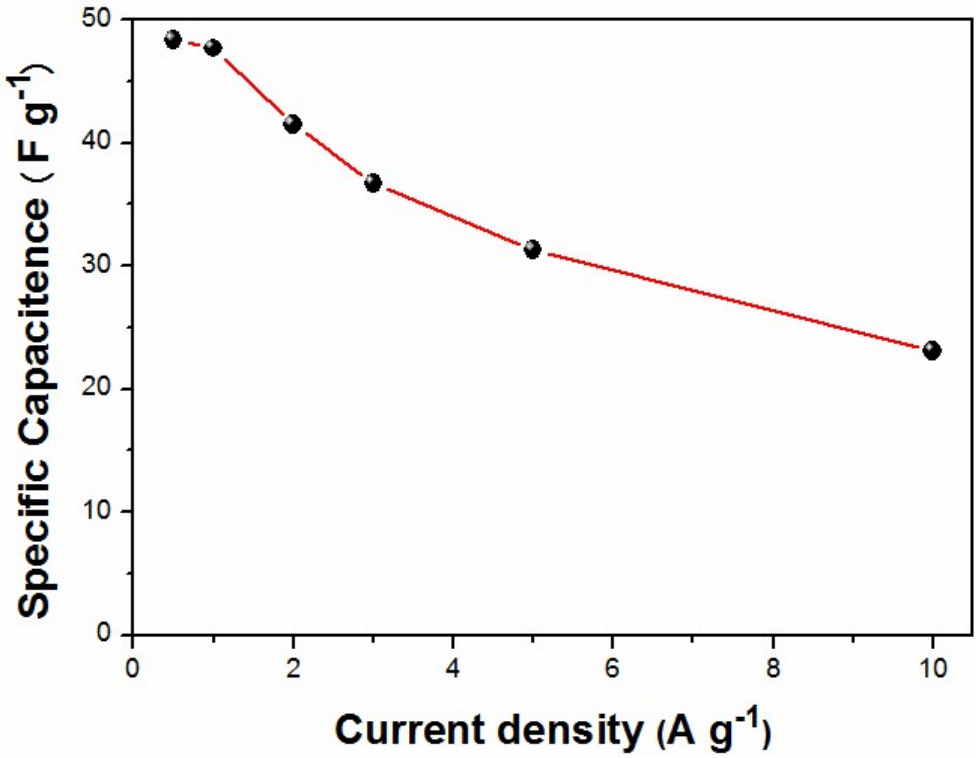

Figure S37. Specific capacity of SNNU-52//AC ASC at various current densities.